Received: 27 May 2019 | Revised: 16 December 2020 | Accepted: 18 December 2020

IET Generation, Transmission & Distribution

DOI: 10.1049/gtd2.12118

The Institution of Engineering and Technology WILEY

ORIGINAL RESEARCH PAPER

A non-linear adaptive excitation control scheme for feedback linearized synchronous generations in multimachine power systems

Tushar Kanti Roy[1] | **Md. Apel Mahmud**[1] | **Weixiang Shen**[2] | **Amanullah Maung Than Oo**[1]

[1] Electrical Power and Energy Systems Research Lab (EPESRL), School of Engineering, Deakin University, Waurn Ponds, Victoria, Australia

[2] School of Software and Electrical Engineering, Swinburne University of Technology, Hawthorn, Victoria, Australia

Correspondence
Md. Apel Mahmud, Electrical Power and Energy Systems Research Lab (EPESRL), School of Engineering, Deakin University, Waurn Ponds, VIC 3216, Australia.
Email: apel.mahmud@deakin.edu.au

Abstract

A new adaptive scheme is proposed in this paper to design excitation controllers for feedback linearized models of synchronous generators in multimachine power systems in order to ensure the stability during large disturbances. The proposed scheme uses speed deviations of synchronous generators, readily available measured physical properties of multimachine power systems, to make all generators within a power network as partially linearized as well as to provide more damping. An adaptive scheme is then used to estimate all unknown parameters which appear in the partial feedback linearizing excitation controllers in order to avoid parameter sensitivities of existing feedback linearization techniques. The overall stability of multimachine power systems is ensured through the excitation control and parameter adaptation laws. The Lyapunov stability theory is used to theoretically analyse the stability of multimachine power systems with the proposed scheme. Simulation studies are presented to evaluate the performance of the proposed excitation control scheme for two different test systems by different operating conditions including short-circuit faults on key locations along with variations in parameters for a large duration. Furthermore, comparative results are presented to highlight the superiority of the proposed adaptive partial feedback linearizing excitation control scheme over an existing partial feedback linearizing excitation controllers.

1 | INTRODUCTION

Modern power networks are being more complicated due to the expansion of existing networks to meet the increasing power demand along with the integration of renewable energy sources [1]. Such power networks are also being stressed for transferring huge amounts of extra power transfer from generators to consumers and experience oscillations due to either small or large disturbances [2, 3]. These oscillations often persist for a longer period which has significant impacts on the stability of power networks. Furthermore, power networks are highly non-linear as operating points change frequently due to constantly varying load demands. These stability issues can be tackled by excitation systems of synchronous generators as excitation controllers provide additional damping and the overall performance of the system depends on the ability of providing such damping under different operating conditions [4, 5].

Power system stabilizers (PSSs) are commonly used excitation controllers which reduce low-frequency oscillations by providing additional damping into power systems [2]. Several methods have been investigated in [6–9] to design PSSs where these are designed by considering linearized models of power systems. PSSs are effective for small disturbances are very small, e.g. small variations in the operating points from the original equilibrium due to slight changes in customers' demand. Some advanced linear control techniques such as robust H_∞ [10, 11] controller have recently been proposed to design excitation controllers. However, these PSSs are less effective for large disturbances where operating conditions vary over a wide range and examples of such disturbances include short-circuit

faults on key points of power networks, large variations in loads etc. [12].

Non-linear excitation controllers are independent of operating points as these are designed by using non-linear dynamical models of synchronous generators in power networks. Hence, non-linear excitation controllers are fully capable to ensure the stable operation of power networks under changing operating conditions [13–15]. Generally, non-linear excitation controllers are designed using different forms of non-linear feedback linearization schemes [16–18]. Recently, it is found that excitation controllers based on the partial feedback linearization scheme are more effective as compared to other feedback linearizing excitation controllers such as exact feedback linearizing excitation controllers (EFBLECs) and direct feedback linearizing excitation controllers (DFBLECs) in terms of minimizing the oscillations in a quicker way by providing adequate damping torques [19–22]. However, the performance of partial feedback linearizing excitation controllers (PFBLECs) relies on some parameters of synchronous generators which are mostly known as stability sensitive parameters [23, 24]. For example, the Tasmanian power system requires to maintain the minimum threshold level of inertia as 3200 megawatt-seconds (MWs) for operating the system in a satisfactory operating state while this value is 3800 MWs for the secure operating state [25]. As indicated in [25], it can be seen that the inertia requirement of a system changes with fault levels. The same applies for other parameters within the system and hence, the faults within a system change the dynamic characteristics of the system. These existing feedback linearizing excitation control laws are the functions stability sensitive parameters along with some physical properties of synchronous generators and the overall stability of multimachine power systems is severely affected with the variations of these parameters [23, 24]. Since variations of stability sensitive parameters are very common in power systems, for example, the parameters of the generators vary from their nominal values along with changes in overall configurations of power systems when faults occur [26]. Thus, it is essential to design non-linear excitation controllers in such a way that these ensure robustness against variations of these parameters.

Sliding mode excitation controllers are robust against variations in parameters [27, 28]. However, the overall stability of multimachine power systems is confined to sliding surfaces which are quite hard to determine for wide variations of operating points. A simple sliding mode controller (SMC) cannot provide satisfactory performance under variations in parameters as it is assumed that the perturbations are to be bounded during the design process and the prior knowledge of these upper bounds is required to implement the controller. However, it is difficult and even sometime quite impossible to obtain these upper bounds of perturbations. Therefore, a supreme upper bound is chosen to cover the whole range of perturbations. For this reason, the SMC based on this supreme upper bound becomes over-conservative which usually causes a poor tracking performance, undesirable oscillations, and poor response against transients within the system. Moreover, the SMC suffers from steady-state chattering effects, despite good robustness properties, which further deteriorates the stability margin of the system and makes it difficult for the practical implementation.

Adaptive control schemes do not require the selection of upper bounds and thus, overcome the limitations of SMCs. Non-linear adaptive techniques can be used to design excitation controllers where all parameters (including stability sensitive parameters) within the dynamical models of synchronous generators can be modelled as completely unknown and then adaptation laws can be designed to adapt or estimate these parameters [29–32]. A robust adaptive feedback controller is designed in [33] where both angle and voltage stability issues are considered. In [33], the effect of parameter variations from their unperturbed values is quantified through L_2 and L_∞ properties while adaptation laws with the inclusions projection operators are used to estimate unknown parameters. A robust backstepping scheme is employed in [34] by considering all parameters appearing within the dynamical models of synchronous generators in a multimachine power system while considering the effects of external disturbances. However, these adaptation laws are slow which lead to larger settling times for the estimation of unknown parameters. Moreover, the dynamical models are simplified so that the controller requires to stabilize only few states. Recently, higher-order models of synchronous generators in multimachine power systems are used in [35] to design a robust adaptive excitation control scheme in order to provide robustness against parametric uncertainties and external disturbance. Recently, an improved robust non-linear backstepping control scheme is proposed in [36] to design excitation controller for synchronous generators. However, the performance of these parameter adaptation laws highly relies on the selection of adaptation gains. Apart from this, all these adaptive backstepping controllers require to use all states within the system as feedback variables. Hence, it is usually assumed that all states are either directly measurable or can be expressed in terms of measured variables. However, the transient stability of power networks needs to be maintained within a specific timeframe and hence, it is essential to have faster responses which can be obtained by combing adaptive and partial feedback linearization scheme as evidenced from anti-lock braking systems in [37].

The combination of parameter adaptation and feedback linearization scheme is employed in [38] to design new excitation controllers for synchronous generators. The parameter adaptation laws for the adaptive feedback linearizing controller in [38] do not estimate all stability sensitive parameters. In [31], the model of synchronous generators is exploited in neuro-identification and the feedback linearizing controller is designed based on this model and such a model exploitation is very difficult for the real-time operation of large and complex power systems. Therefore, it is essential to design a controller which will consider all stability sensitive parameters appearing in the control laws as unknown and provide faster responses.

As mentioned earlier, the PFBLEC in [19] provides faster responses and does not require any observer to estimate states used for feedback to the controller but it is very sensitive to variations in parameters. From [19], it is evident that excitation control laws include stability sensitive parameters of synchronous generators while including different physical properties of each

generator. These properties mainly include power (both active and reactive), speed deviation, and terminal voltage. On contrary, all stability sensitive parameters in such PFBLECs can be modelled as unknown in order to estimate through parameter adaptation laws and thus, the adaptive control scheme can be incorporated with the partial feedback linearization scheme to tackle the stability of power systems against large disturbances in a faster way while considering different operating conditions.

Based on the literature so far discussed in this work, existing gaps can be summarized as follows:

- The parameter sensitivity issues of feedback linearizing excitation controllers are bounded to some certain values while requiring to satisfy some strict conditions and existing literature do not cover the parameter sensitivity problems without having any relax conditions.
- Existing adaptive backstepping controllers work on the assumption that all states of synchronous generators are somehow measurable though it is not practically feasible. It is essential to have additional observers to make it practically feasible.
- Since existing adaptive excitation controllers use estimated values of parameters, the response time of these controllers is usually slow.

This paper aims to cover these gaps by utilizing the benefits of both partial feedback linearizing and adaptive controllers. This paper contributes to design adaptive partial feedback linearizing excitation controllers (APFBLECs) for synchronous generators in multimachine power systems. The main contribution of this paper with respect to existing key literature can be summarized as follows:

- The partial feedback linearization scheme is used in this work which transforms the dynamical model of a synchronous generator into a lower order one as compared to the original system as presented in [3, 19]. This work is different from [3, 19] in the sense that the proposed adaptive partial feedback linearization scheme is designed for the feedback linearized models as discussed in [19]. However, the proposed scheme is also applicable for the model in [3]. Such feedback linearized models are independent of operating points and help to ensure faster dynamic performance.
- The parameters appearing within the feedback linearized model of the synchronous generator in a multimachine power system are considered as unknown in order to avoid the estimation of unnecessary or all parameters as presented in [34, 35] and thus, the convergence speed becomes more faster than existing adaptive controllers.
- The proposed scheme overcomes the parameter sensitivity problems of the existing partial feedback linearization scheme and overestimation of parameters in the existing adaptive controllers.

The performance of the proposed scheme is evaluated on two test systems: (i) the two-area four-machine power system and (ii) the three-area seven-machine 29-bus power system. Simulation results are carried out under to enure the applicability of the proposed scheme on different test systems while considering different operating conditions. Furthermore, the superiority of APFBLECs are analysed over an EPBLEC.

2 | DYNAMICAL MODELLING OF MULTIMACHINE POWER SYSTEMS

The design and implementation of the proposed control scheme requires to select an appropriate mathematical model of multimachine power systems with conventional synchronous generators. As the main purpose here is to design and implement excitation controllers, it is assumed that the power network equipped with the synchronous generators is connected through long transmission lines and other equipments to supply loads. Synchronous generators in multimachine power systems are commonly represented as third-order models for the design and implementation of excitation controllers and such representations are mostly known as the direct-axis transient reactance behind a voltage source [2]. The dynamical models considered in this section are applicable to any number of synchronous generators in a multimachine power system. In this work, it is considered that there are n synchronous generators, the mathematical model of ith synchronous generator is represented through the following set of non-linear dynamical equations [2, 19]:

Generator mechanical dynamics:

$$\begin{aligned}\dot{\delta}_i &= \omega_i - \omega_{0i}\\ \dot{\omega}_i &= -\frac{D_i}{2H_i}(\omega_i - \omega_{0i}) + \frac{\omega_{0i}}{2H_i}(P_{mi} - P_{ei}).\end{aligned} \tag{1}$$

Generator electrical dynamics:

$$\dot{E}'_{qi} = \frac{1}{T_{doi}}(E_{fdi} - E_{qi}). \tag{2}$$

Electrical equations of ith synchronous generators:

$$E_{qi} = E'_{qi} - (x_{di} - x'_{di})I_{di}, \tag{3}$$

$$P_{ei} = {E'_{qi}}^2 G_{ii} + E'_{qi}\sum_{\substack{j=1\\ j\neq i}}^{n} E'_{qj}B_{ij}\sin\delta_{ij}, \tag{4}$$

$$Q_{ei} = -{E'_{qi}}^2 G_{ii} - E'_{qi}\sum_{\substack{j=1\\ j\neq i}}^{n} E'_{qj}B_{ij}\cos\delta_{ij}, \tag{5}$$

$$I_{qi} = E'_{qi}G_{ii} + \sum_{\substack{j=1\\ j\neq i}}^{n} E'_{qj}B_{ij}\sin\delta_{ij}, \tag{6}$$

$$I_{di} = -E'_{qi}G_{ii} - \sum_{\substack{j=1\\ j\neq i}}^{n} E'_{qj}B_{ij}\cos\delta_{ij}, \tag{7}$$

$$V_{ti} = \sqrt{(E'_{qi} - x'_{di} I_{di})^2 + (x'_{di} I_{qi})^2}. \tag{8}$$

All electrical equations, i.e. Equations (3)–(8) can be substituted into Equations (1)–(2) in order to obtain the complete dynamical model of ith synchronous generator which can be expressed as follows:

$$\begin{aligned}
\dot{\delta}_i &= \omega_i - \omega_{0i} \\
\dot{\omega}_i &= -\frac{D_i}{2H_i}\left(\omega_i - \omega_{0i}\right) + \frac{\omega_{0i}}{2H_i} P_{mi} - \frac{\omega_{0i}}{2H_i}\left(E'^{2}_{qi} G_{ii} \right. \\
&\quad \left. + E'_{qi} \sum_{j=1 j\neq i}^{n} E'_{qj} B_{ij} \sin \delta_{ij}\right) \\
\dot{E}'_{qi} &= -\frac{1 + (x_{di} - x'_{di}) B_{ii}}{T_{doi}} E'_{qi} + \frac{(x_{di} - x'_{di})}{T_{doi}} \\
&\quad \sum_{j=1 j\neq i}^{n} E'_{qj} B_{ij} \cos \delta_{ij} + \frac{1}{T_{doi}} E_{fdi}.
\end{aligned} \tag{9}$$

The first step of designing the proposed excitation controller is to obtain the partial feedback linearized models of synchronous generators in multimachine power systems as discussed in the following section.

3 | PARTIAL FEEDBACK LINEARIZED MODELS OF MULTIMACHINE POWER SYSTEMS

The non-linear dynamical model of any synchronous generator in a multimachine power system as represented by Equation (9) can be expressed as a generalized non-linear dynamical system as shown by the following equation [19]:

$$\begin{aligned}
\dot{x} &= f(x) + g(x)u \\
y &= h(x).
\end{aligned} \tag{10}$$

The output functions $y = h(x)$ defines the feedback linearizability of the non-linear dynamical model in Equation (10). It is found in [39] that the power system model becomes exactly linearized if the rotor angle is selected as the output and the selection of the speed deviation transforms the system into a partially linearized one.

The feedback linearization technique decouples a multimachine power system into several subsystems depending on the number of excitation control inputs (which in turn reflects the number of synchronous generators) in a multimachine power system [19]. This means that there will be n partial feedback linearized subsystems as there are n synchronous generators in a multimachine power system [19]. For the multimachine power system in this paper, each partially linearized subsystem can be written as [19]:

$$\dot{z}_{1i} = z_{2i}, \tag{11}$$

$$\dot{z}_{2i} = L^2_{fi} h_i(x_i) + L_{gi} L^1_{fi} h_i(x_i) u_i, \tag{12}$$

where the subscript $i = 1, 2, \cdots, n$ is used to represent the number of subsystem, the superscript L represents the Lie derivative, and

$$\begin{aligned}
L^2_{fi} h_i(x_i) &= -\frac{D_i}{2H_i}\Delta\dot{\omega}_i - \frac{\omega_{0i}}{2H_i} Q_{ei} \Delta\omega_i - \frac{\omega_{0i}}{2H_i} P_{ei}, \\
L_{gi} L^1_{fi} h_i(x_i) &= -\frac{\omega_{0i}}{T_{doi} 2H_i} \frac{P_{ei}}{E_{qi}}.
\end{aligned}$$

By substituting $L^2_{fi} h_i(x_i)$ and $L_{gi} L^1_{fi} h_i(x_i)$ into Equation (12), it can be written as follows:

$$\dot{z}_{1i} = z_{2i}, \tag{13}$$

$$\begin{aligned}
\dot{z}_{2i} &= -\frac{D_i \omega_{0i}}{4H_i^2} P_{mi} + \frac{D_i^2}{4H_i^2}\Delta\omega_i + \frac{D_i \omega_{0i}}{4H_i^2} P_{ei} - \frac{\omega_{0i}}{2H_i} \\
&\quad (Q_{ei}\Delta\omega_i + P_{ei}) - \frac{\omega_{0i}}{T_{doi} 2H_i} \frac{P_{ei}}{E_{qi}} u_i.
\end{aligned} \tag{14}$$

Equations (13) and (14) can be simplified as follows:

$$\begin{aligned}
\dot{z}_{1i} &= z_{2i}, \\
\dot{z}_{2i} &= v_i,
\end{aligned} \tag{15}$$

where v_i is a linear control law which can be written as

$$\begin{aligned}
v_i &= -\frac{D_i \omega_{0i}}{4H_i^2} P_{mi} + \frac{D_i^2}{4H_i^2}\Delta\omega_i + \frac{D_i \omega_{0i}}{4H_i^2} P_{ei} \\
&\quad - \frac{\omega_{0i}}{2H_i}(Q_{ei}\Delta\omega_i + P_{ei}) - \frac{\omega_{0i}}{T_{doi} 2H_i} \frac{P_{ei}}{E_{qi}} u_i.
\end{aligned} \tag{16}$$

Equation (15) is the partially linearized model of ith synchronous generator connected to a multimachine power system. The original control law u_i can be obtained from Equation (16) and implemented by choosing v_i as any linear controller. The implementation of such controllers requires the stability analysis of the internal dynamics which is not repeated here as the detailed analysis is presented in [19]. However, the excitation control law is the function of stability sensitive parameters D_i, H_i, and T_{doi} of synchronous generators. The adaptive control problem is formulated based on the sensitiveness of these parameters.

4 | PARAMETER SENSITIVITY ANALYSIS AND MODELLING OF STABILITY SENSITIVE PARAMETERS

If the parameters of synchronous generators, which appear in the control law as represented in Equation (16) are varied, the

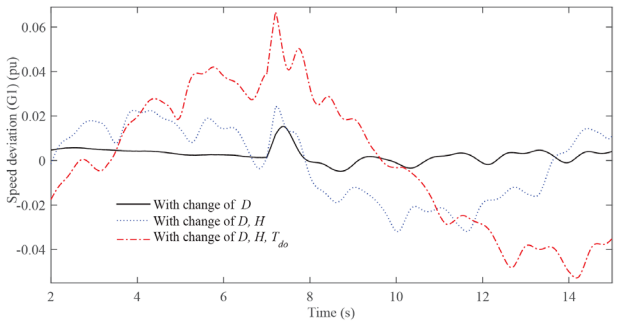

FIGURE 1 Speed deviation of G1 with variations in stability sensitive parameters while applying a three-phase short-circuit fault at the terminal of the generator G1

stability margin of power systems will be affected. When only one parameter, e.g. the damping co-efficient (D_i) is slightly varied (here it is reduced by 10%) from its nominal value, i.e. $D_i = 4$; the stability of the whole system will be disturbed as shown in Figure 4. The sensitivity of this variation can be seen from in Figure 1 where the speed deviation (solid black line) of the first synchronous generator (G1) is shown while an EPF-BLEC is employed and the terminal of G1 is considered as a point to apply the three-phase short-circuit fault.

Figure 1 clearly depicts that the speed deviation of G1 has oscillating characteristics with the variation of D_i, but it becomes unstable (dotted blue line) when both D_i and inertia constant (H_i) are changed from their nominal values. The stability margin of the system degrades more (dash-dotted red line) when all three parameters D_i, H_i, and T_{doi} are varied. As mentioned earlier, these parameters usually vary during the practical operations of power systems and it is quite impossible to directly know the exact values of these parameters due to continuously changing operational characteristics of power systems. For example, the parameter T_{doi} is the function of the direct-axis transient reactance and it is quite impossible to know the exact value of this parameter. Here, the nominal values of H and T_{do} for G1 are considered as 6.5 and 8, respectively, and to perform this simulation, these values have been reduced by 10%.

Similarly, the actual values of D_i and H_i cannot be known. If the parameters D_i, H_i, and T_{doi} are considered as unknown, the following expressions can be obtained from Equation (16):

$$\theta_{1i} = -\frac{D_i}{4H_i^2}P_{mi},\ \theta_{2i} = \frac{D_i^2}{4H_i^2},\ \theta_{3i} = \frac{D_i}{4H_i^2}$$
$$\theta_{4i} = -\frac{1}{2H_i},\ \text{and}\ \theta_{5i} = -\frac{1}{T_{doi}2H_i}, \tag{17}$$

where θ_{ji} with $j = 1, 2, 3, 4, 5$ are stability sensitive parameters which need to be estimated through the adaptation laws for the design and implementation of the proposed adaptive excitation controller on multimachine power systems. These stability sensitive parameters as modelled through Equation (17) can be incorporated within the partial feedback linearized model of multimachine power systems in Equations (13)–(14) and rewritten as follows:

$$\dot{z}_{1i} = z_{2i}, \tag{18}$$

$$\dot{z}_{2i} = \omega_{0i}\theta_{1i} + \Delta\omega_i\theta_{2i} + \omega_{0i}P_{ei}\theta_{3i} + \theta_{4i}(Q_{ei}\Delta\omega_i + P_{ei})$$
$$\omega_{0i} + \theta_{5i}\frac{\omega_{0i}P_{ei}}{E_{qi}}u_i. \tag{19}$$

The proposed adaptive excitation control scheme is developed based on the model in Equation (18) and the following section presents the detailed controller design process.

5 | PROPOSED APFBLEC DESIGN

The main target in this section is to design the excitation control law u_i in order to ensure the transient stability of power systems during large disturbances while providing robustness against stability sensitive parameters. The proposed non-linear adaptive scheme has the ability to steer z_{1i} (ω_i, speed) to its desired value z_{1id} (ω_{0i}, synchronous speed). To achieve this, z_{2id} is determined to stabilize Equation (18) and finally, u_i to stabilize Equation (19) which in turn stabilizes the whole system. The following steps elaborately discuss the design procedure of the proposed excitation control scheme.

Step 1: Determination of z_{2id}

According to the design purpose, the first error variable for the model in Equation (18) can be written as

$$e_{1i} = z_{1i} - z_{1di} \tag{20}$$

whose derivative can be written as

$$\dot{e}_{1i} = \dot{z}_{1i} = z_{2i}, \tag{21}$$

where z_{2i} is actually the second state variable in Equation (18) and it can be considered as a virtual control variable to stabilize $\dot{e}_{1i}$. The error of this second state will be analysed in the next step and its corresponding error variable can be defined as

$$e_{2i} = z_{2i} - z_{2di}. \tag{22}$$

The insertion of Equation (22) into Equation (21) yields

$$\dot{e}_{1i} = e_{2i} + z_{2di}, \tag{23}$$

where z_{2id} is an equivalent variable corresponding to z_{2i} as $z_{2i} = z_{2id}$ when $e_{2i} = 0$. Hence, it can be considered as a stabilizing function (i.e. a virtual control law) which is used to temporarily stabilize the error dynamic in Equation (23). For analysing the stability of this error dynamic, the control Lyapunov function (CLF) as per the Lyapunov stability theory can be written as

$$W_{1i} = \frac{1}{2}e_{1i}^2 \tag{24}$$

and its derivative along the trajectory, after inserting Equation (23), can be written as

$$\dot{W}_{1i} = e_{1i}\dot{e}_{1i} = e_{1i}(e_{2i} + z_{2di}). \tag{25}$$

For stabilizing the error dynamic in Equation (23), z_{2id} should be chosen in such a manner that $\dot{W}_{1i}$ becomes negative definite or negative semi-definite, i.e. $\dot{W}_{1i} < 0$ or $\dot{W}_{1i} \leq 0$. Any state-feedback controller, as indicated in the following, can be used to stabilize this situation.

$$z_{2di} = -k_{1i}e_{1i}, \tag{26}$$

where k_{1i} represents a positive constant design parameter and used to ensure the faster convergence of e_{1i}. The state feedback controller in Equation (26) simplifies Equation (25) as

$$\dot{W}_{1i} = -k_{1i}e_{1i}^2 + e_{1i}e_{2i}. \tag{27}$$

From Equation (27), it can be seen that its negative semi-definiteness depends on the error e_{2i} appearing in the second terms on the right-hand side which will be cancelled in the following step. Hence, the final decision for the overall stability of the system is not made in this step. However, it is essential to calculate the time derivative of z_{2di} as it will be used in the next step which can be written as

$$\dot{z}_{2di} = -k_{1i}\dot{e}_{1i} = -k_{1i}z_{2i}. \tag{28}$$

The remaining error dynamic is analysed in the next step while determining the excitation control and parameters adaptation laws.

Step 2: Calculation of u_i

The dynamics of e_{2i} in Equation (22) can be written as

$$\dot{e}_{2i} = \dot{z}_{2i} - \dot{z}_{2di}. \tag{29}$$

The values of $\dot{z}_{2i}$ from Equation (19) and $\dot{z}_{2di}$ from Equation (28) can be substituted into Equation (29) which will yield

$$\begin{aligned}\dot{e}_{2i} = {} & \omega_{0i}\theta_{1i} + \Delta\omega_i\theta_{2i} + \omega_{0i}P_{ei}\theta_{3i} + \theta_{4i}(Q_{ei}\Delta\omega_i + P_{ei}) \\ & \omega_{0i} + \theta_{5i}\frac{\omega_{0i}P_{ei}}{E_{qi}}u_i + k_{1i}z_{2i}.\end{aligned} \tag{30}$$

Since θ_{1i}, θ_{2i}, θ_{3i}, θ_{4i}, and θ_{5i} are unknown parameters; it is possible to rewrite Equation (30) as follows by assuming $\hat{\theta}_{1i}$, $\hat{\theta}_{2i}$, $\hat{\theta}_{3i}$, $\hat{\theta}_{4i}$, and $\hat{\theta}_{5i}$ are their corresponding estimated values.

$$\begin{aligned}\dot{e}_{2i} = {} & \omega_{0i}\hat{\theta}_{1i} + \omega_{0i}(\theta_{1i} - \hat{\theta}_{1i}) + \Delta\omega_i\hat{\theta}_{2i} + k_{1i}z_{2i} \\ & + \Delta\omega_i(\theta_{2i} - \hat{\theta}_{2i}) + \omega_{0i}P_{ei}\hat{\theta}_{3i} + \omega_{0i}P_{ei}(\theta_{3i} - \hat{\theta}_{3i}) + \\ & \omega_{0i}(Q_{ei}\Delta\omega_i + P_{ei})\hat{\theta}_{4i} + \omega_{0i}(Q_{ei}\Delta\omega_i + P_{ei}) \\ & (\theta_{4i} - \hat{\theta}_{4i}) + \hat{\theta}_{5i}\frac{\omega_{0i}P_{ei}}{E_{qi}}u_i + \frac{\omega_{0i}P_{ei}}{E_{qi}}u_i(\theta_{5i} - \hat{\theta}_{5i}).\end{aligned} \tag{31}$$

The excitation control input appears in Equation (31) which needs to be obtained in a manner that all errors converge to zero, i.e. $e_{1i} \to 0$ and $e_{2i} \to 0$ as $t \to \infty$. With the control law u_i to stabilize the errors e_{1i} and e_{2i} related to the dynamics as represented by Equations (18) and (19), the final CLF can be chosen as

$$\begin{aligned}W_{2i} = {} & W_{1i} + \frac{1}{2}e_{2i}^2 + \frac{1}{2\gamma_{1i}}(\theta_{1i} - \hat{\theta}_{1i})^2 \\ & + \frac{1}{2\gamma_{2i}}(\theta_{2i} - \hat{\theta}_{2i})^2 + \frac{1}{2\gamma_{3i}}(\theta_{3i} - \hat{\theta}_{3i})^2 \\ & + \frac{1}{2\gamma_{4i}}(\theta_{4i} - \hat{\theta}_{4i})^2 + \frac{1}{2\gamma_{5i}}(\theta_{5i} - \hat{\theta}_{5i})^2,\end{aligned} \tag{32}$$

where γ_{mi} with $m = 1, 2, 3, 4, 5$ is a positive scalar which is called adaptation gain. The convergence of the estimation error depends of the values of these adaptation gains and the convergence rate is higher when the values of these gains are set to larger values. However, the cost will be increased for larger values of these adaptation gains. Therefore, the optimum values of these gains need to be selected for achieving the desired control objectives. In this paper, these values are selected to ensure the transient stability of the power system within 2 s after the clearance of the faults as this is the standard time for power system stability analysis [2].

The time derivative of W_{2i} is

$$\begin{aligned}\dot{W}_{2i} = {} & \dot{W}_{1i} + e_{2i}\dot{e}_{2i} - \frac{1}{\gamma_{1i}}(\theta_{1i} - \hat{\theta}_{1i})\dot{\hat{\theta}}_{1i} - \frac{1}{\gamma_{2i}}(\theta_{2i} \\ & - \hat{\theta}_{2i})\dot{\hat{\theta}}_{2i} - \frac{1}{\gamma_{3i}}(\theta_{3i} - \hat{\theta}_{3i})\dot{\hat{\theta}}_{3i} - \frac{1}{\gamma_{4i}} \\ & (\theta_{4i} - \hat{\theta}_{4i})\dot{\hat{\theta}}_{4i} - \frac{1}{\gamma_{5i}}(\theta_{5i} - \hat{\theta}_{5i})\dot{\hat{\theta}}_{5i}.\end{aligned} \tag{33}$$

Substituting $\dot{W}_{1i}$ from Equation (27) and $\dot{e}_{2i}$ from Equation (31) into Equation (33) yields

$$\begin{aligned}\dot{W}_{2i} = {} & -k_{1i}e_{1i}^2 + e_{2i}(e_{1i} + \omega_{0i}\hat{\theta}_{1i} + \Delta\omega_i\hat{\theta}_{2i} + \omega_{0i}P_{ei}\hat{\theta}_{3i} \\ & + \omega_{0i}\left(Q_{ei}\Delta\omega_i + P_{ei})\hat{\theta}_{4i} + \hat{\theta}_{5i}\frac{\omega_{0i}P_{ei}}{E_{qi}}u_i + k_{1i}z_{2i}\right) \\ & - (\theta_{1i} - \hat{\theta}_{1i})\gamma_{1i}^{-1}(\dot{\hat{\theta}}_{1i} - \gamma_{1i}e_{2i}\omega_{0i}) - (\theta_{2i} - \hat{\theta}_{2i})\gamma_{2i}^{-1} \\ & (\dot{\hat{\theta}}_{2i} - \gamma_{2i}e_{2i}\Delta\omega_i) - (\theta_{3i} - \hat{\theta}_{3i})\gamma_{3i}^{-1}(\dot{\hat{\theta}}_{3i} - \omega_{0i}\gamma_{3i}e_{2i}P_{ei}) \\ & - (\theta_{4i} - \hat{\theta}_{4i})\gamma_{4i}^{-1}(\dot{\hat{\theta}}_{4i} - \gamma_{4i}e_{2i}(Q_{ei}\Delta\omega_i + P_{ei})) \\ & - (\theta_{5i} - \hat{\theta}_{5i})\gamma_{5i}^{-1}\left(\dot{\hat{\theta}}_{5i} - \gamma_{5i}e_{2i}\frac{P_{ei}\omega_{0i}u_i}{E_{qi}}\right).\end{aligned} \tag{34}$$

The influences of unknown terms $(\theta_{1i} - \hat{\theta}_{1i})$, $(\theta_{2i} - \hat{\theta}_{2i})$, $(\theta_{3i} - \hat{\theta}_{3i})$, $(\theta_{4i} - \hat{\theta}_{4i})$, and $(\theta_{5i} - \hat{\theta}_{5i})$ in $\dot{W}_{2i}$ can be eliminated selecting the adaptation laws as follows:

$$\dot{\hat{\theta}}_{1i} = \gamma_{1i}e_{2i}\omega_{0i}, \tag{35}$$

$$\dot{\hat{\theta}}_{2i} = \gamma_{2i} e_{2i} \Delta\omega_i, \tag{36}$$

$$\dot{\hat{\theta}}_{3i} = \omega_{0i} \gamma_{3i} e_{2i} P_{ei}, \tag{37}$$

$$\dot{\hat{\theta}}_{4i} = \gamma_{4i} e_{2i} \omega_{0i} (Q_{ei} \Delta\omega_i + P_{ei}), \tag{38}$$

$$\dot{\hat{\theta}}_{5i} = \gamma_{5i} e_{2i} \frac{P_{ei} \omega_{0i} u_i}{E_{qi}}. \tag{39}$$

Here, the adaptation laws are selected in a manner so that $\dot{W}_{2i}$ becomes negative semi-definite for which the whole system becomes stable and the final error converges to zero. As a result, Equation (34) can be simplified as

$$\dot{W}_{2i} = -k_{1i} e_{1i}^2 + e_{2i}(e_{1i} + \omega_{0i}\hat{\theta}_{1i} + \Delta\omega_i \hat{\theta}_{2i} + \omega_{0i} P_{ei} \hat{\theta}_{3i} + \omega_{0i}(Q_{ei}\Delta\omega_i + P_{ei})\hat{\theta}_{4i} + \hat{\theta}_{5i} \frac{\omega_{0i} P_{ei}}{E_{qi}} u_i + k_{1i} z_{2i}). \tag{40}$$

The time derivative of W_2 should be negative definite or semi-definite as this would ensure the overall stability of the whole power system which is still not reflected in Equation (40). However, this can be achieved if the original excitation control law is selected as follows:

$$u_i = -\frac{E_{qi}}{\hat{\theta}_{5i}\omega_{0i} P_{ei}} (e_{1i} + \omega_{0i}\hat{\theta}_{1i} + \Delta\omega_i \hat{\theta}_{2i} + \omega_{0i} P_{ei} \hat{\theta}_{3i} + \omega_{0i}(Q_{ei}\Delta\omega_i + P_{ei})\hat{\theta}_{4i} + k_{2i} e_{2i} + k_{1i} z_{2i}). \tag{41}$$

The substitution of Equation (41) into Equation (40) leads to

$$\dot{W}_{2i} = -k_{1i} e_{1i}^2 - k_{2i} e_{2i}^2 \leq 0, \tag{42}$$

where the values of k_{1i} and k_{2i} are positive tuning parameters. The settling times for the responses (i.e. different physical properties) of the system depend on the values of these parameters and these need to be selected in a way that their corresponding steady-state values are obtained as soon as the faults or disturbances are cleared. From Equation (42), it is clear that the $\dot{W}_{2i}$ is negative definite or semi-definite which indicates the overall stability of the whole multimachine power system.

Equation (41) is the final excitation control law and Figure 2 shows the summary of the whole controller design process which also provides an idea associated with the implementation of the designed controller. Based on this diagram, the overall controller design procedure can be discussed through the following points:

- Obtain and present dynamical models of power networks in the form of generalized non-linear systems;
- Linearize the power system model using partial feedback linearization;
- Obtain the excitation control law from partially linearized system;

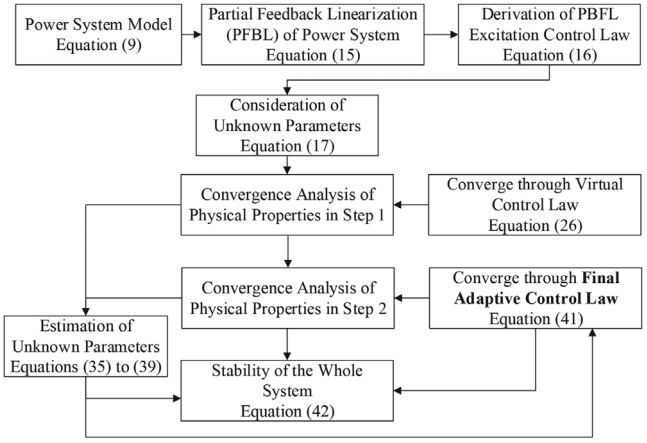

FIGURE 2 Summary of the design process for the APFBLEC

- Consider the parameters of synchronous generator, which appear in the control law, as unknown;
- Analyse the convergence of speed deviation and other relevant physical properties through virtual control law;
- Form a CLF to ensure that the system is stable with the adaptation gains, estimated parameters, and final adaptive control law, and
- Obtain the final control law and check the overall stability with this law.

The designed APFBLEC is practically feasible and it can be implemented on any synchronous generator within a multimachine power system as the proposed partial feedback linearization scheme decouples the system. From Equation (41), it can be seen that all variables except E_{qi} are directly measurable while all unknown parameters associated with the system can be obtained adaptation laws in Equations (35)–(39). The q-axis voltage of the synchronous generator can also be represented in terms of measured variables as discussed in [19] and thus, it can be said that all variables in Equation (41) are either directly measurable or can be expressed in terms of measured variables. The control law in Equation (41) also includes gain parameters which are selected in a trial and error approach. At the same time, adaptation laws in Equations (35)–(39) use adaptation gains and directly measurable variables where these adaptation gains are also selected based on a trial and error method. It is worth noting that the control law in Equation (41) does not include any information of other synchronous generators except the generator on which it will be employed. Hence, the designed controller uses only the local information of synchronous generators on which it will be implemented. It has further been clarified in the implementation block diagram of the designed controller as shown in Figure 3.

From the implementation block diagram as shown in Figure 3, it can be seen that the excitation control law for the designed APFBLEC will adapt the changes within the system where such changes may appear due to transient characteristics, e.g. changes in load demands (i.e. operating conditions), network topologies due to faults etc. The main reason behind having

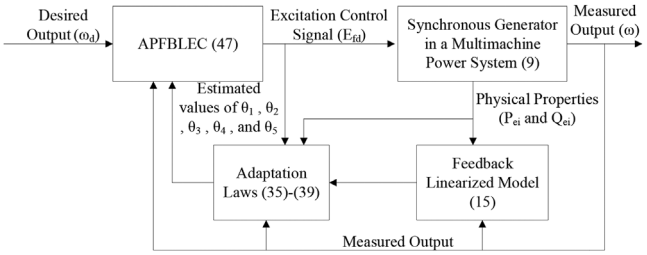

FIGURE 3 Implementation block diagram of the APFBLEC

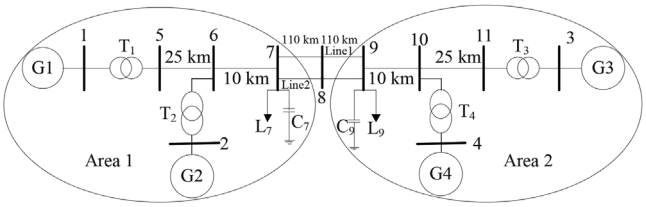

FIGURE 4 Test system: a two-area network with four machines and 11-bus

such an adaptation capability is that the controller uses online measurements where all changes are reflected through measurements. Since the designed controllers require only local measurements, it does not rely on any communication that might degrade the reliability of the system. Furthermore, the generation unit operator does not require to know the information associated with changes in the system in order to feed into the controller as the controller directly captures the changes through measurement. Having said this, the performance of the designed controller might be affected by other generators if these are strongly coupled. In such situations, it is essential to use distributed control schemes that allow to use information of neighbouring generators. However, this is out of the scope of this paper as it is quite normal that synchronous generators in multimachine power system supplying a large geographical area are weekly coupled. The performance of the designed excitation controller as represented by Equation (41) and adaptation laws in Equations (35)–(39) is evaluated in the following section by considering two different multimachine power systems.

6 | PERFORMANCE EVALUATION OF THE DESIGNED EXCITATION CONTROLLER

Two test systems: (i) a two-area system with four machines and 11-bus and (ii) three-area seven-machine 29-bus system are used in this paper for evaluating the effectiveness of the designed controller during different types of large disturbances. In both test systems, synchronous generators are mainly modelled as transient level generators (GENTRA) except for the infinite bus. The synchronous generator at the infinite bus is modelled as a classical generator (GENCLS). During the simulation of the system using the designed and existing excitation controllers, a physical limit of ±6 pu is used for all excitation systems. The more detailed case studies are presented in the following two subsections.

6.1 | Performance evaluation on a two-area test system with four machines and 11-bus

The configuration of the first test system, i.e. the two-area power system with four machines and 11-bus as presented in Figure 4 is used to demonstrate the performance of the designed APFBLEC controller. There are four synchronous generators within this test system and the second one, i.e. G2 is considered as the slack or infinite bus and therefore, it is modelled as a GENCLS. As mentioned earlier, other synchronous generators (G1, G3, and G4) are considered as GENTRAs. The parameters of generators, transmission lines, and loads can be found in [2]. Modal analyses have been performed to identify the effects of each synchronous generator on the overall stability of the system. From modal analyses, it is identified that G1 and G3 are more sensitive for affecting the overall stability of the system as compared to other generators. Thus, the designed APFBLECs are employed with the excitation systems of G1 and G3 in order to obtain a cost-effective solution. The following five cases are considered to validate the performance of the designed controller:

1. The application of a symmetrical short-circuit (which is also refereed three line-to-ground, i.e. 3LG) fault on the key location, i.e. at the terminal of the most sensitive generator, i.e. G3
2. The temporary tripping of a key transmission line for affecting the power transfer between two areas, i.e. the line between bus-8 and bus-9
3. The permanent disconnection of one transmission line between two areas, i.e. between bus-8 and bus-9
4. The inclusion of noises with the mechanical power inputs to the most sensitive generators, i.e. G1 and G3
5. Variations in parameters

All these case studies are considered to demonstrate the operational capability of the system under different operating conditions. In this work, it is considered that all transient events occurs at $t = 7$ s. For the cases of the temporary fault or tripping of a line, the duration of 0.2 s is considered. This means that the short-circuit fault is applied at $t = 7$ s and cleared after 0.2 s, i.e. at t=7.2 s. The same situation is considered for the temporary tripping of the line where the line is reconnected at $t = 7.2$ s. For the third case, the line is permanently disconnected at $t = 7$ s while the noise for the fourth case is applied the same instant, i.e. at $t = 7.2$ s. The parameter variations for the final case is also considered from $t = 7$ s. An EPFBLEC as discussed in [19] is used to compare the results obtained from the designed APFBLEC under all these cases. The results are also compared with an existing PSS as presented in [7].

- **Case 1: Application of a symmetrical short-circuit fault on a key location, i.e. at the terminal of G3**

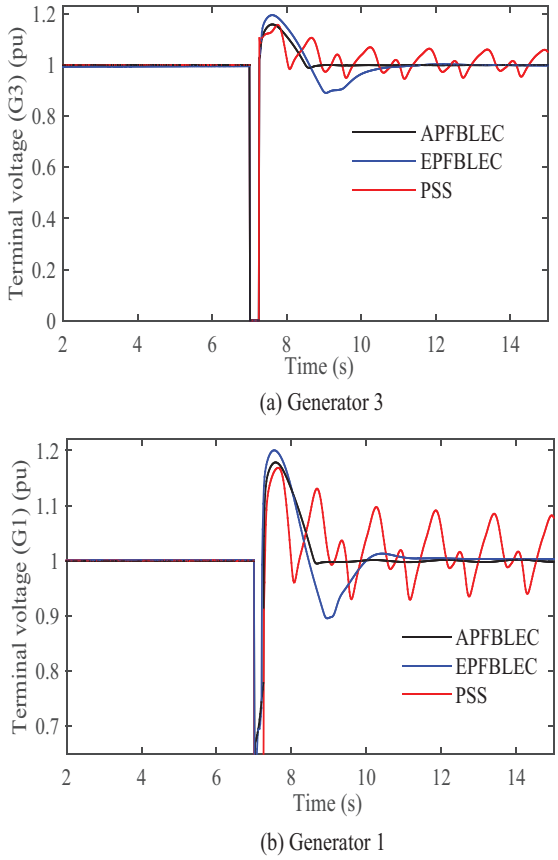

FIGURE 5 Terminal voltages of G3 and G1 for Case 1

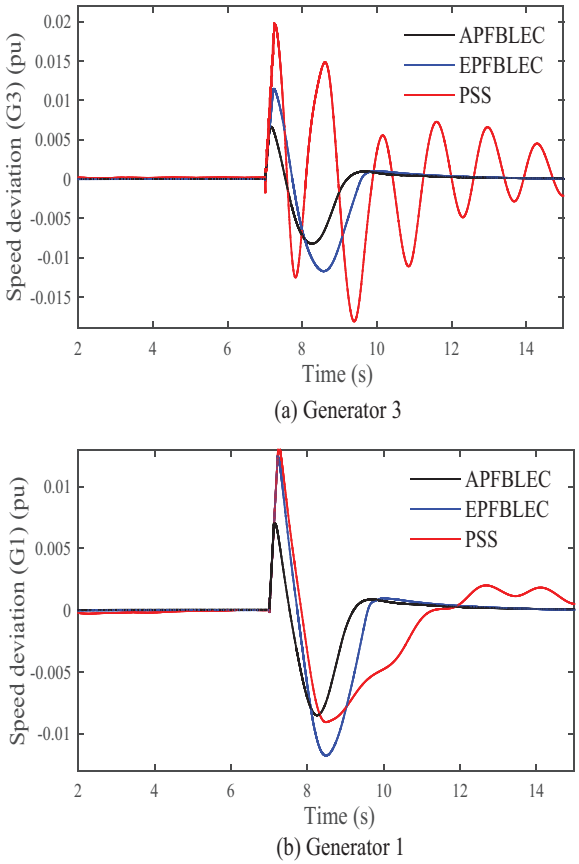

FIGURE 6 Speed deviations of G3 and G1 for Case 1

A symmetrical short-circuit fault, i.e. a 3LG fault, at the connection point of G3 which indicates the terminal, can be considered as the most severe fault as this generator is sensitive to the overall stability of the two-area test system. Initially, the terminal voltage of this generator is in the steady state and it is disturbed due to the application of this fault at $t = 7$ s. This terminal voltage becomes zero for the duration of the fault, i.e. from $t = 7$ s to $t = 7.2$ s which can also be seen from Figure 5(a). However, the main point of interest is the post-fault terminal voltage of G3 along with the same for other stability sensitive generation within the system which is G1 for this test system. The settling time of the terminal voltage for G3 depends on the effectiveness of the excitation controller. From Figure 5(a), it can be observed that the designed APFBLEC quickly settles the terminal voltage response (black line) of G3 to its pre-fault steady-state value as compared to the EPFBLEC (blue line). The terminal voltage of G3 with the PSS is also shown in Figure 5(a) (red line) which does not settle and this indicates that the PSS is unable to ensure the stability. The impact of this fault on G1 is shown through its terminal voltage as presented in Figure 5(b) which clearly depicts that the terminal voltage is affected. However, the terminal voltage of G1 does not become zero during the fault condition. From Figures 5(a) and (b), it is obvious that the APFBLEC (black line) provides excellent damping torque as compared to the EPFBLEC (blue line) and PSS (red line).

Usually, the speed deviation for the synchronous generator is always zero as it operates at the synchronous speed, i.e. the measured speed and desired or nominal speed are same which have been clearly reflected for both G3 and G1 with the designed APFBLEC and EPFBLEC as shown in Figures 6(a) and (b), respectively. The speed deviation responses for both G3 and G1 are disturbed during the fault condition. However, the desired speed deviation, i.e. zero speed deviation is achieved after clearing the fault though the convergence speed of the designed controller is much quicker than that of the existing controller. So, it is evident that the designed controller (black line) provides better performance in terms of settling time and oscillation damping than the EPFBLEC (blue line) and PSS (red line).

Figures 7(a) and (b) show the corresponding rotor angles of generators G3 and G1, respectively. The rotor angles in these figures change which will destabilize the whole system unless a proper control action is initiated to settle down the system to its initial operating conditions. From Figures 7(a) and (b), it is clear that the post-fault responses are similar to initial, i.e. pre-fault responses when the designed APFBLEC (black line) is used. However, the post-fault responses still have oscillations with larger amplitudes and take longer time to reach their initial values when the EPFBLEC (blue line) is used. On the other hand, PSS (red line) shows more oscillating characteristics with a tendency to reduce the amplitude of oscillations. The active power and control signals also settle down to their pre-fault

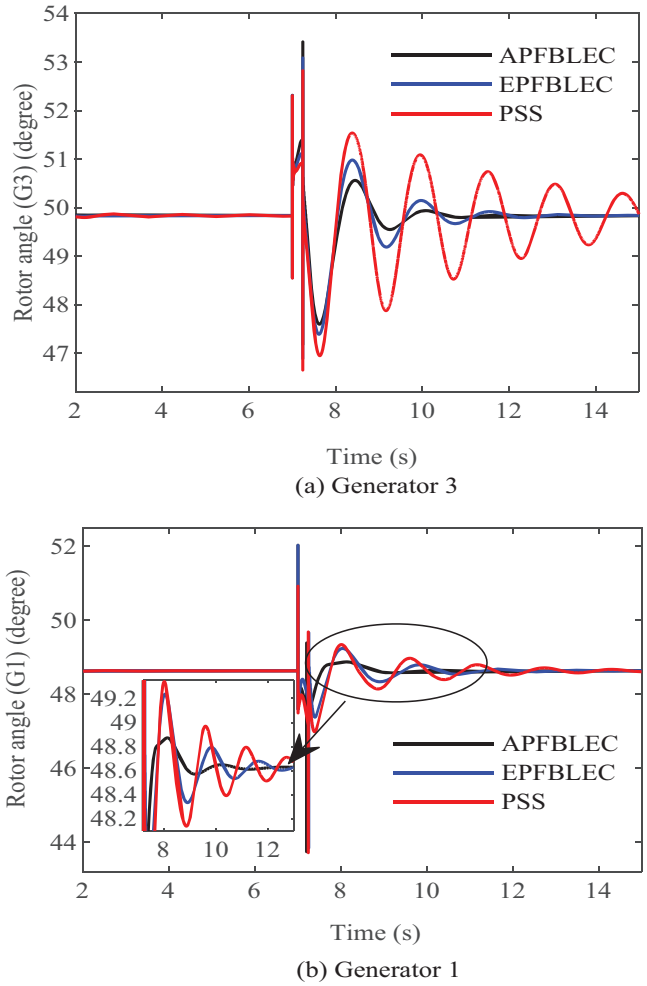

FIGURE 7 Rotor angles of G3 and G1 for Case 1

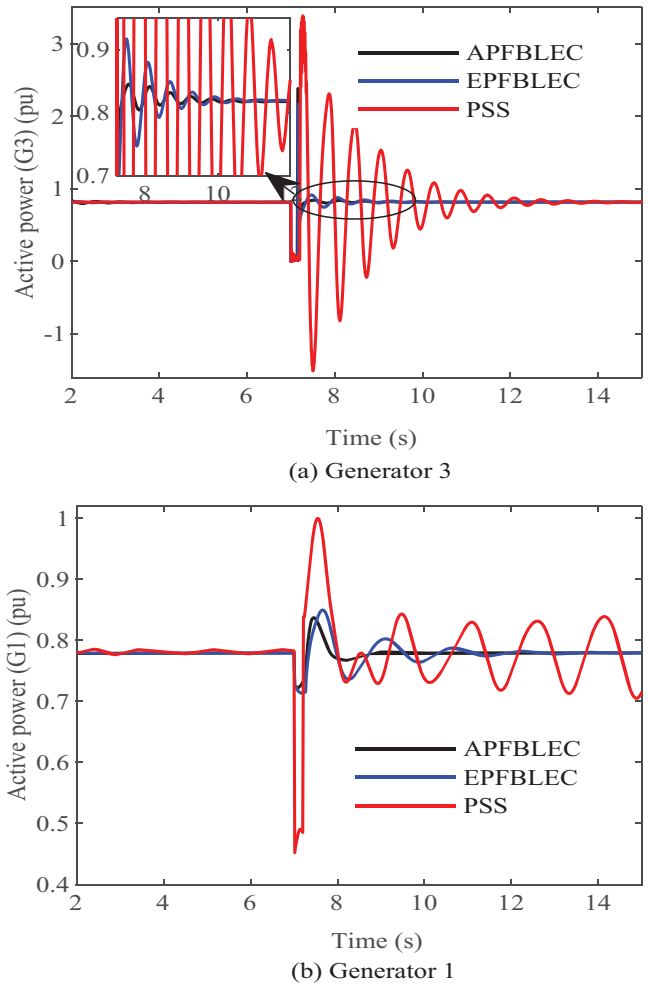

FIGURE 8 Output active power of G3 and G1 for Case 1

values after clearing the fault as depicted in Figures 8 and 9, respectively. Thus, it is very clear that the designed APFBLEC controller responds in a quicker manner than the existing controllers. Adaptation laws are used to estimate stability sensitive unknown parameters which are shown in Figure 10 from where it is clearly demonstrated that these parameters converge to their nominal values within the timescale of maintaining the transient stability, i.e. within few cycles after clearing the fault. The convergence time of these parameters is quite similar to that of other responses of the system. This clearly shows the parameter estimation capability of the designed APFBLEC along with faster settling time. The percentage overshoot in the terminal voltage, speed deviation, rotor angle, and output active power for G3 and G1 are shown in Tables 1 and 2, respectively, from where it can be clearly seen that the designed APFBLEC performs better than the EPFBLEC and PSS. It is also worth noting that the settling time for the PSS is not even comparable with the designed controller.

It is clear that the designed AFPBLEC ensures the stable operation of the two-area power system while a severe short-circuit fault is applied. The main reason behind ensuring such a stable operation is the damping capability of the controller during severe faults. The controller directly captures the changes in the terminal voltage, active power, reactive power, and speed deviation which can also be evidenced from the changes in the control signal as shown in Figure 9. The parameter estimation process at the beginning shows some oscillations which have been stabilized within 1.5 s and these oscillations appear due to the selection of the initial values of unknown parameters. However, adaptation laws help estimated parameters to reach their original values that ensure the steady-state operation of the whole system. Hence, the designed controller ensures the desired damping into the system by continuously adapting the changes within the system through online measurements.

- **Case 2: The temporary tripping of a key transmission line for affecting the power transfer between two areas, i.e. the line between bus-8 and bus-9**

There are two parallel transmission lines (line-1 and line-2) between bus-8 and bus-9 in Figure 4 which connect area-1 with area-2 for exchanging power from one area to another. The line-2 is tripped for a duration of 0.2 s which will affect the power transfer and this can be clearly seen from the power flowing

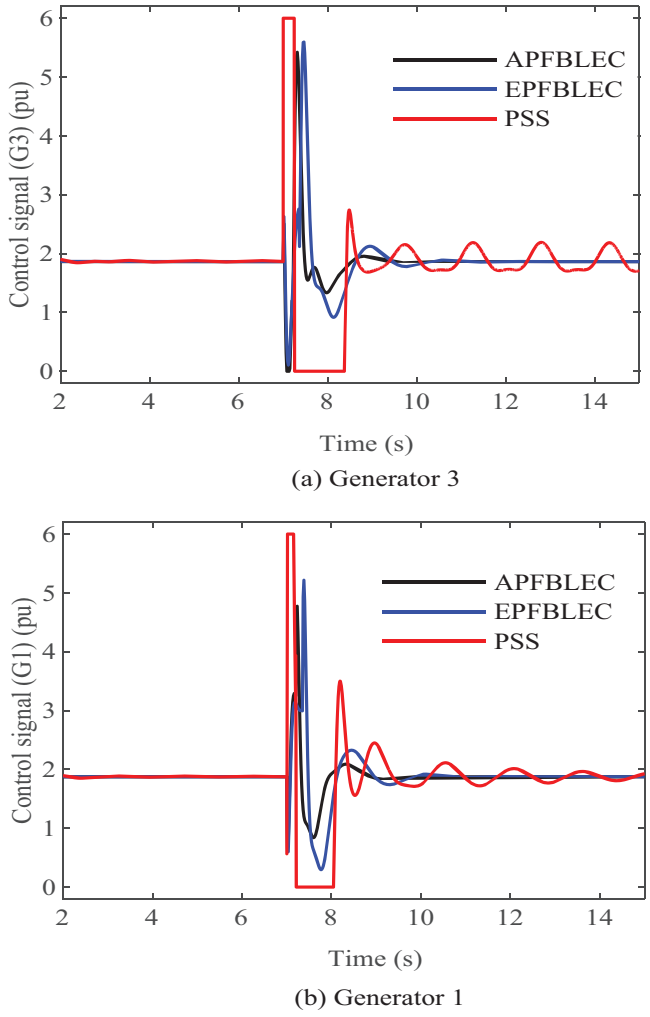

FIGURE 9 Excitation control signals of G3 and G1 for Case 1

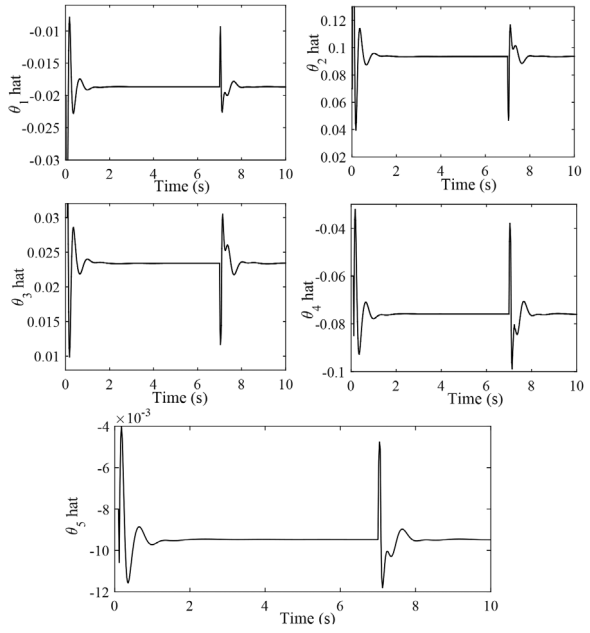

FIGURE 10 Estimated unknown parameters for Case 1

through the line as presented in Figure 11(a). From this figure, it is observed that the power flowing through line-2 becomes zero from $t = 7$ s to $t = 7.2$ s, i.e. during the period for which line-2 is tripped. However, line-1 becomes overloaded during this tripped period as this line carries the excess power for exchanging desired power between two areas which can also be clearly seen from Figure 11(b). In this work, it is assumed that line-1 has the ability to carry the excess power which is not generally the case during the practical operation and it is assumed to demonstrate the overloading condition of the line. From Figure 11, it can be seen that there exist oscillations after reconnecting the line. Figure 11 also clearly depicts that the power

TABLE 1 Percentage overshoot and settling time for different responses of G3 for Case 1

	Percentage overshoot				Settling time (s)			
Control technique	Terminal voltage	Speed deviation	Rotor angle	Active power	Terminal voltage	Speed deviation	Rotor angle	Active power
APFBLEC	13.3	0.67	1.44	6.58	1.4	2.30	3.36	0.37
EPFBLEC	19.5	1.28	2.29	14.58	3.62	2.68	5.34	1.28
PSS	15.30	1.30	3.33	185.62	∞	∞	∞	5.2

TABLE 2 Percentage overshoot and settling time for different responses of G1 for Case 1

	Percentage overshoot				Settling time (s)			
Control technique	Terminal voltage	Speed deviation	Rotor angle	Active power	Terminal voltage	Speed deviation	Rotor angle	Active power
APFBLEC	17	0.64	1.17	6.70	1.5	2.15	2.06	0.82
EPFBLEC	19.90	1.13	1.27	9.91	3.78	2.72	4.87	3.67
PSS	17.20	1.96	1.44	28.2	∞	∞	6.67	∞

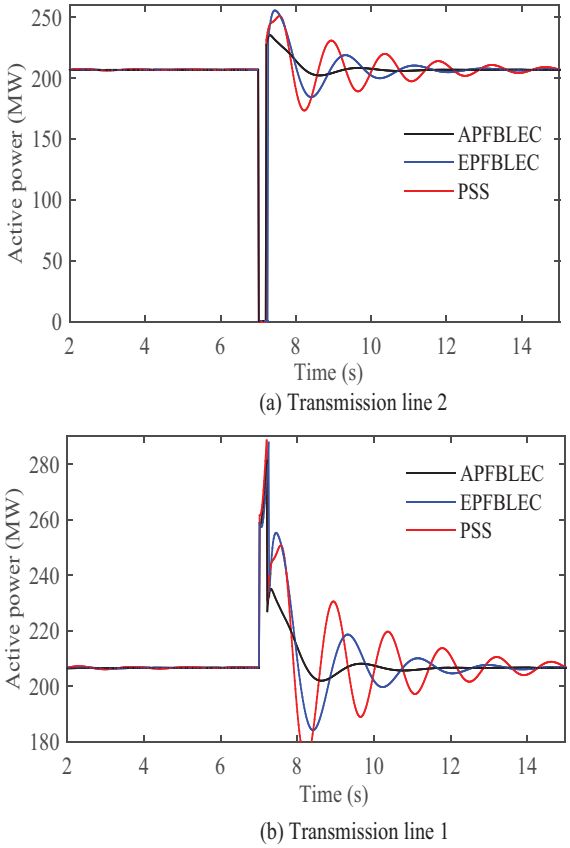

FIGURE 11 Active power flowing between two areas through line-1 and line-2 between bus-8 and bus-9 for Case 2

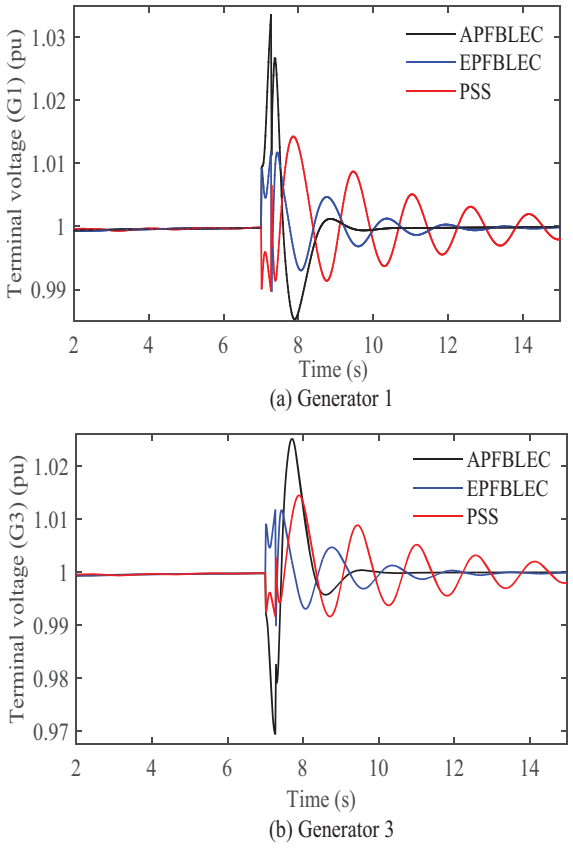

FIGURE 12 Terminal voltages of G1 and G3 for Case 2

flowing through these two lines quickly settle to their initial values when the tripped line is reconnected through the recloser action at $t = 7.2$ s and the designed APFBLEC outperforms the EPFBLEC as oscillations are less with the designed controller and thus, clearly shows enhanced damping characteristics.

Figures 12(a) and (b) show the pre-fault and post-fault terminal voltages of generators G1 and G3 with both the proposed controller (black line) and existing controllers (blue and red line). The terminal voltage responses in these figures exhibit some oscillations during the period for which line-2 is tripped. However, the severity of the oscillations on the terminal voltage is less as the voltage stability issue is not prominent for tripping the transmission line. It can be seen that the designed APFBLEC improves the voltage stability as compared to existing controllers due to better the damping capability.

Both APBLEC and EPFBLEC ensure the synchronous operations of synchronous generators which can be seen from speed deviations in Figures 13(a) and (b) as the zero speed deviation is maintained with these controllers. However, the speed deviations for both G1 and G3 are highly oscillating when the PSS is used. From Figure 13, it can be seen that the speed deviation of G3 includes more oscillations as compared to that of G1. However, the oscillations in the speed deviations are damped within the few cycles after clearing the fault when the designed APFBLEC which is not the case for the EPFBLEC and PSS. Furthermore, the amplitudes of oscillations in the speed deviations for both G1 and G3 are higher with the EPFBLEC these do not even settle down to their desired values with the PSS. Figures 14(a) and (b) show the rotor angle responses of G1 and G3, respectively, from where it can be seen that the severity of oscillations in these responses are much higher than other responses, e.g. the terminal voltage and speed deviation. This is mainly due to the fact that the changes in the active power responses are strictly coupled with the changes in the rotor angles of synchronous generators. Figure 14 clearly demonstrates that the post-fault rotor angles with the APFBLEC quickly settle to their initial pre-fault values as compared to the EPFBLEC and PSS. The control signals also reflect similar characteristics which can be found from Figure 15. From the control signals of both G1 and G3 in Figure 15, it can be seen that the amplitudes of oscillations are initially high with the designed controller as compared to the EPFBLEC but much better than the PSS. However, the designed controllers for both G1 and G3 ensure the faster settling time. Tables 3 and 4 include the percentage overshoot of all responses associated with the terminal voltage, speed deviation, and rotor angle of G1 and G3, respectively. Table 4 also includes the same for the power flowing through line-1 and line-2. The percentage overshoot and settling time in these tables clearly demonstrate the superiority of the designed APFBLEC over the existing EPFBLEC and PSS.

- **Case 3: The permanent disconnection of line-2 between bus-8 and bus-9**

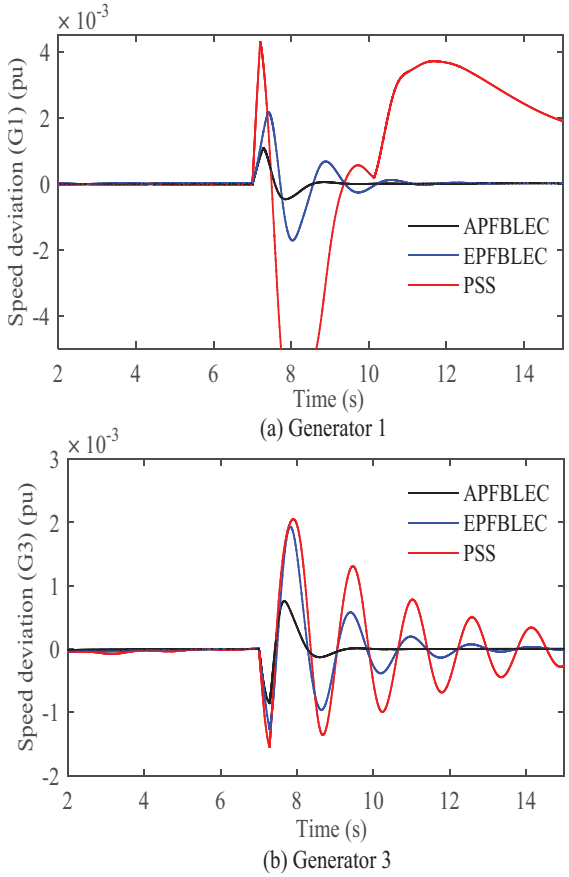

FIGURE 13 Speed deviations of G1 and G3 for Case 2

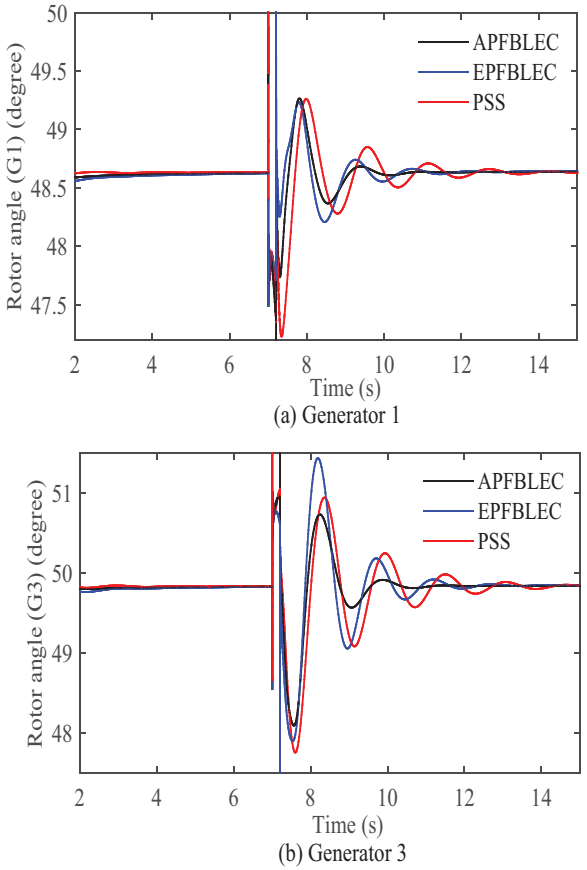

FIGURE 14 Rotor angles of G1 and G3 for Case 2

In this case, the transmission line-2 is permanently disconnected from the system in order to demonstrate the operational feature of the system under stressed conditions as it is considered that all generators are still generating the same power. In this situation, there will be no power flowing through the transmission line-2 as shown in Figure 16(b). However, the excess power, which was flowing through line-2, will be flowing through transmission line-1 as depicted in Figure 16(a). The active power response experiences more oscillations with the existing controller as compared to the designed controller which can also be found in Figure 16(a). It seems that the existing controllers are unable to properly handle the situation and thus, the oscillations still persist for a longer duration and the PSS is not even able to damp these oscillations. The similar situations have been reflected in the control signals as shown in Figure 17 from where it can be seen that the control signals for both G1 and G3 show oscillation for a very long period with the existing controllers. The operation of the system with such oscillations may lead to the unstable operation. However, this is not the case with the designed controller. The percentage overshoot and the settling time for active power flowing through line-1 are shown in Table 5 from where it can be seen that APFBLEC has the lowest percentage overshoot and settling time. Furthermore, the settling time for the PSS is too long while it is reasonable for the EPFBLEC.

- **Case 4: Inclusion of noises with the mechanical power inputs of G1 and G3**

During the practical operation of power systems, some measurement noises appear to the mechanical power input of the turbine-governor system which is coupled with the synchronous generator. But feedback linearization technique has the capability to decouple noises and therefore, if there is any external noise into the system; the controller will decouple the noise from the system to achieve the desired control objectives [3, 40].

The simulation results in this case study are obtained by incorporating external noises with the measured mechanical power inputs of both G1 and G3. In this work, the measurement noises are considered as white Gaussian noises and these noises do severely affect the overall performance of the system. With the inclusion of these noises, the physical properties of G1 and G3 such as terminal voltages, speed deviations, rotor angles, and active power outputs of the generators change slightly which are shown from Figures 18 to 21, respectively. These changes last for only few seconds as the designed controller has very good noise decoupling capability. The main reason of having improved noise decoupling capability as compared to traditional, i.e. EPFBLEC is that the designed controller adapts these noises and cancels during the negative impacts of these noises. The control signals are also shown in Figure 22

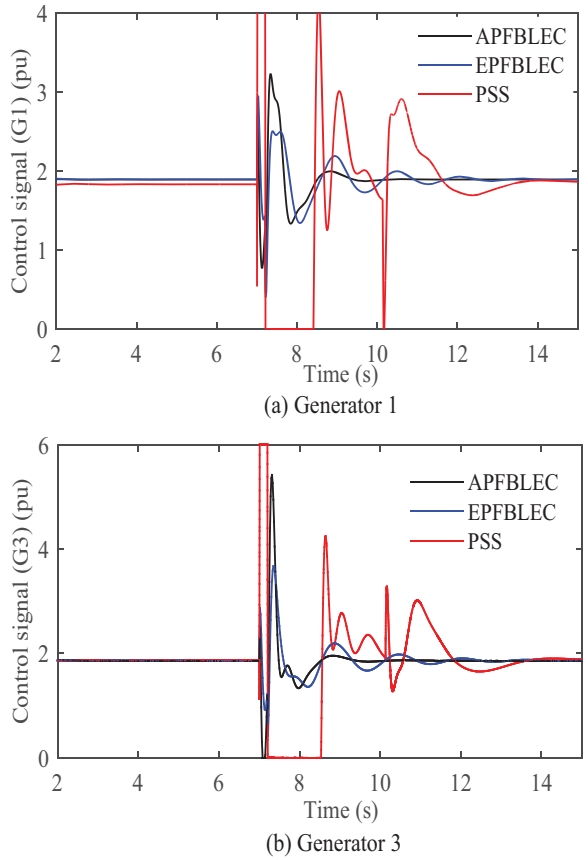

FIGURE 15 Control signals of G1 and G3 for Case 2

which clearly reflect that the designed APFBLEC exhibits more stable characteristics as compared to the existing controllers. The designed controller overcomes the severity of noises and hence, improves the overall stability. However, the PSS exhibits continuously oscillating behaviours in all these responses as it does not have the ability to provide robustness against such noises. The performance characteristics are quantified in terms of the percentage overshoot and settling time for different responses of G1 and G3 which are shown in Tables 6 and 7, respectively. From these tables, it can be clearly seen that the APFBLEC performs better than the EPFBLEC and PSS in all aspects.

The critical clearing angle (CCA) is considered as an important parameter for analysing the transient stability of power systems. Table 8 shows the CCAs for G3 and G1 for all four cases so far discussed in this section when the designed controller is applied. This table clearly demonstrates that the designed controller ensures extended CCA and enlarges the stability margin.

- **Case 5: Controller performance with variations in parameters**

This case study is carried out to demonstrate the effectiveness of the designed controller with variations in parameters as such variations are common while considering the real-time operations of power grids. The simulation results in this case study are obtained by varying all parameters appearing in the EPFBLEC such as the damping coefficient (D), inertia constant (H), and direct-axis open-circuit time constant (T_{do}) of the generator (G1) from their nominal values. The corresponding speed deviation of G1 is shown in Figure 23 with both designed (APFBLEC) and existing (EPFBLEC) controllers. From Figure 23, it can be seen that the speed deviation changes with variations in parameters when the existing controller is used. However, the speed deviation is slightly affected with the designed APFBLEC when the parameters are perturbed from their original values. The comparisons of the performance between existing

TABLE 3 Percentage overshoot and settling time for different responses of G1 for Case 2

	Percentage overshoot			Settling time (s)			
Control technique	Terminal voltage	Speed deviation	Rotor angle	Terminal voltage	Speed deviation	Rotor angle	
APFBLEC	2.70	0.11	1.17	1.20	1.91	1.40	2.3
EPFBLEC	1.10	0.20	1.27	1.25	4.63	3.67	3.62
PSS	1.40	0.42	1.44	1.30	12.8	∞	5.25

TABLE 4 Percentage overshoot and settling time for different responses of G3 and active power flow through line-1 and line-2 for Case 2

	Percentage overshoot					Settling time (s)				
Control technique	Terminal voltage	Speed deviation	Rotor angle	Active power line-1	Active power line-2	Terminal voltage	Speed deviation	Rotor angle	Active power line-1	Active Power line-2
APFBLEC	2.4	0.07	1.74	13.59	15	2.2	1.58	2.68	2.45	1.65
EPFBLEC	1.2	0.19	3.14	22.80	23.78	4.73	5.75	4.66	5.48	3.55
PSS	1.5	0.20	2.18	20.50	21.35	12	∞	5.92	8.8	6.4

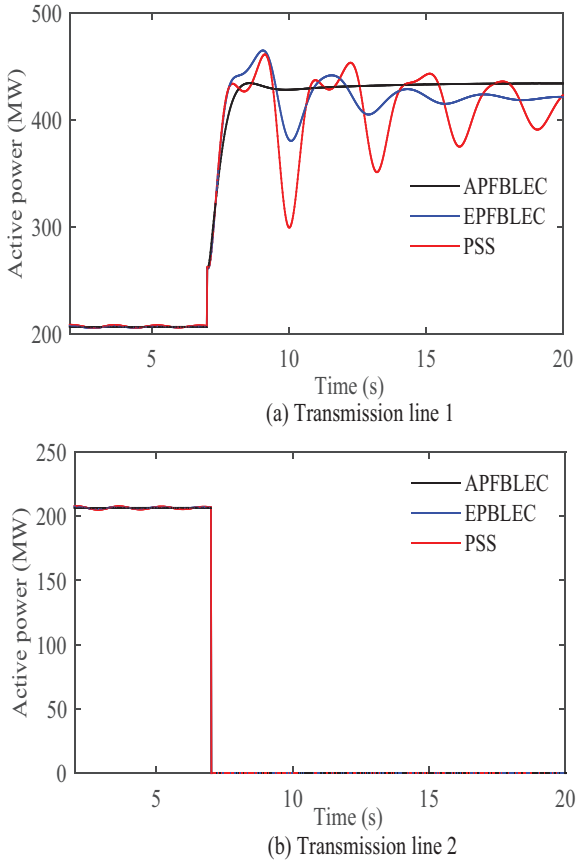

FIGURE 16 Active power flowing from area-1 to area-2 through line-1 and line-2 between bus-8 and bus-9 for Case 3

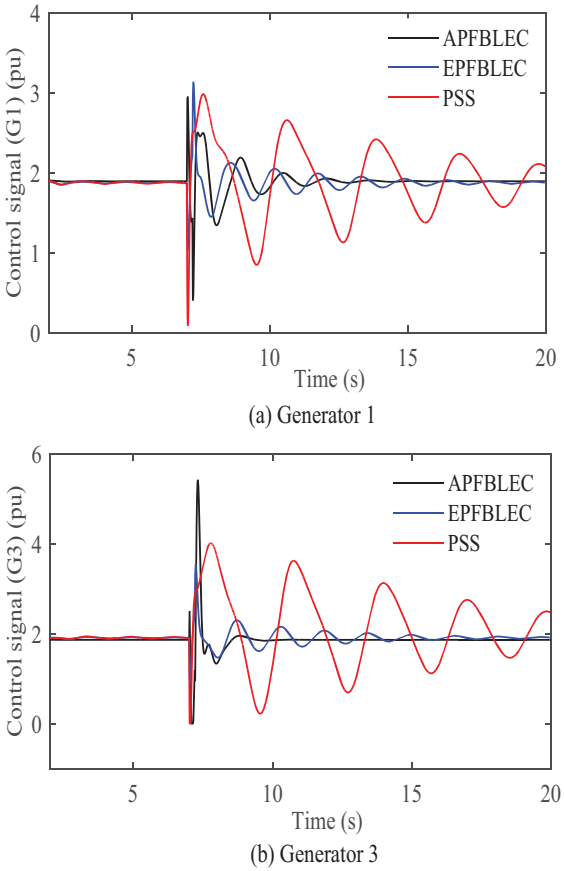

FIGURE 17 Control signals of G1 and G3 for Case 3

TABLE 5 Percentage overshoot and settling time for active power flowing through line-1 for Case 3

Control technique	Percentage overshoot	Settling time (s)
APFBLEC	1.16	1.68
EPFBLEC	1.68	8.43
PSS	8.20	∞

and designed controllers are also shown in Table 9 in terms of percentage variations in parameters, settling time, and system status.

Simulation results under different variations in operating conditions clearly demonstrate that the designed APFBLEC exhibits better performance in terms of providing adequate damping into the system and faster settling time while providing robustness against parametric uncertainties. A large and more realistic test system is considered to further investigate the superiority and suitability of the designed controller as compared to the existing controller and briefly discussed in the following subsection.

6.2 | Performance evaluation on a three-area seven machine 29-bus power system

At this point, it is evident that the designed controller performs well under different operating conditions. In this subsection, a three-area seven machine 29-bus test system as shown in Figure 24 is used to validate the effectiveness of the designed controller as this is a large system compared to the previous test system. This test system consists of a 735 kV transmission network with seven 13.8 kV power plants. The loads are lumped at two buses: bus-17 and bus-18. The load connected to the bus-18 comprises four types of load blocks which are connected with 25 kV distribution system through 735 kV/230 kV and 230 kV/25 kV transformers. The entire system can be divided into three areas such as (i) North-West network (G1-G4), (ii) North-East network (G6-G7), and (iii) Generator G5. The proposed controllers are equipped with G2, G3, G4, G5, G6, and G7 as G1 is considered as the reference generator, i.e. infinite bus. Since three-phase short-circuit faults are the most severe faults in power systems, the simulation results are provided here only for this type of fault though the performance is evaluated for all other cases as discussed in the previous subsection.

From the modal analysis of this test system, it is found that G4 has the most severe impact on the stability of this system and the effect of G3 is slightly less as compared to G4. Therefore, the fault is applied at the terminal of G4 while all

TABLE 6 Percentage overshoot and settling time for different responses of G1 for Case 4

	Percentage overshoot				Settling time (s)			
Control technique	**Terminal voltage**	**Speed deviation**	**Rotor angle**	**Active power**	**Terminal voltage**	**Speed deviation**	**Rotor angle**	**Active power**
APFBLEC	0.90	0.038	0.15	1.03	0.92	1.06	1.05	1.10
EPFBLEC	1.20	0.15	1.48	1.00	2	5.16	2.36	4.3
PSS	3.20	0.70	0.01	2.27	∞	∞	7.44	∞

TABLE 7 Percentage overshoot and settling time for different responses of G3 for Case 4

	Percentage overshoot				Settling time (s)			
Control technique	**Terminal voltage**	**Speed deviation**	**Rotor angle**	**Active power**	**Terminal voltage**	**Speed deviation**	**Rotor angle**	**Active power**
APFBLEC	1.40	0.04	3.26	7.16	1.36	1.28	1.98	1.54
EPFBLEC	1.25	0.16	4.21	10.38	4.62	5.30	5.25	3.08
PSS	3.80	0.71	5.07	7.69	∞	∞	∞	12

TABLE 8 Critical clearing angle (CCA) for G3 and G1 in the two-area power system

Case	**Generator**	**CCA**
1	G3	61.36°
	G1	65.12°
2	G3	120.89°
	G1	141.16°
3	G3	142.68°
	G1	146.48°
4	G3	55.70°
	G1	53.45°

TABLE 9 Parameter sensitivity of the APFBLEC and EPFBLEC

Changes in parameters (%)	**Type of controller**	**Settling time (s)**	**System status**
Nominal	APFBLEC	1.80	stable
	EPFBLEC	2.5	stable
5% variation	APFBLEC	1.85	stable
	EPFBLEC	3	stable
8% variation	APFBLEC	2	stable
	EPFBLEC	5	stable
12% variation	APFBLEC	2.1	stable
	EPFBLEC	∞	Oscillating

responses are taken for G3 and G4. For this test system, a similar fault sequence, which is similar to the previous subsection (i.e. the fault occurs at $t = 7$ s and clears at 7.2 s), is considered. The terminal voltages, speed deviations, and rotor angles

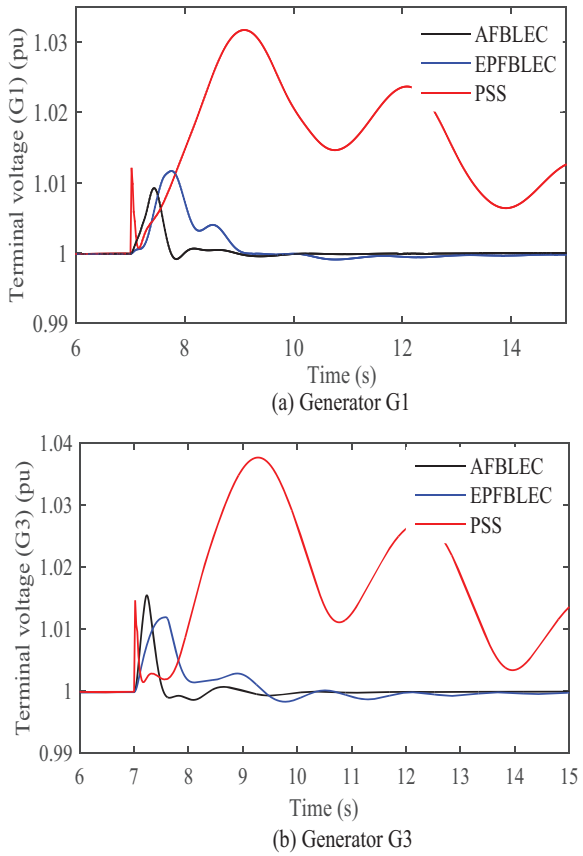

FIGURE 18 Terminal voltages of G1 and G3 with external noises to mechanical power inputs of these generators

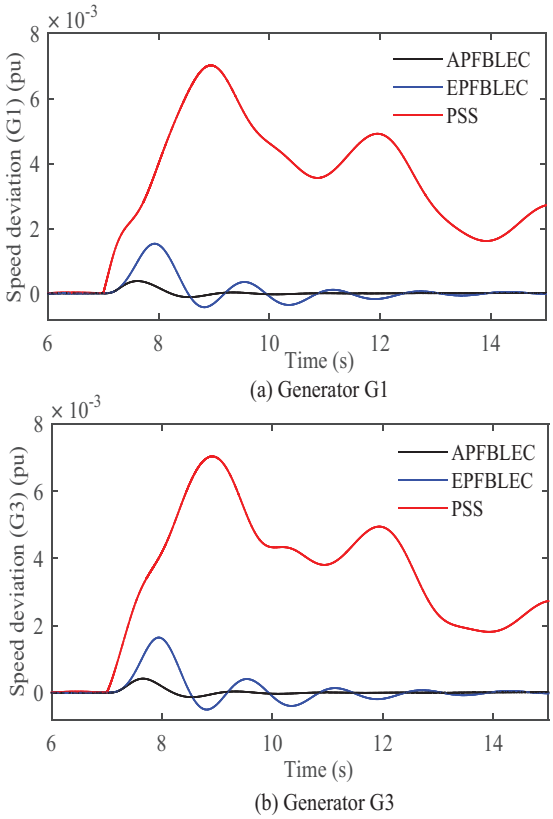

FIGURE 19 Speed deviations of G1 and G3 with external noises to mechanical power inputs of these generators

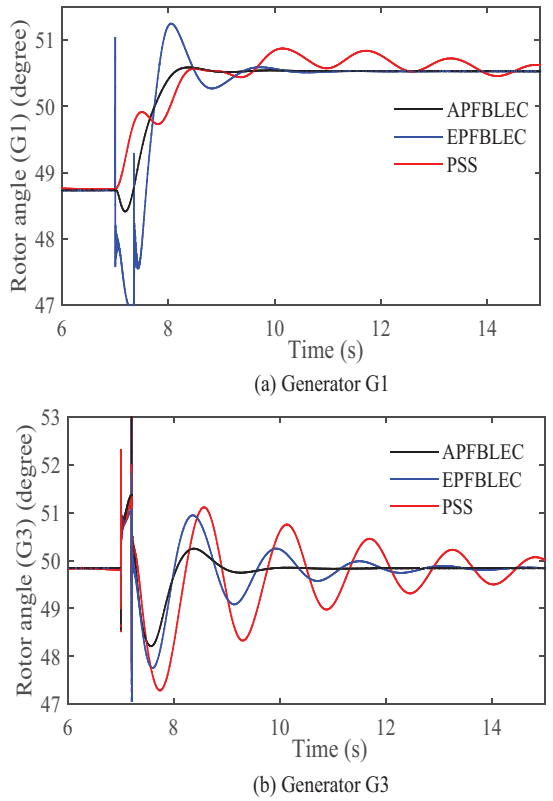

FIGURE 20 Rotor angles of G1 and G3 with external noises to mechanical power inputs of these generators

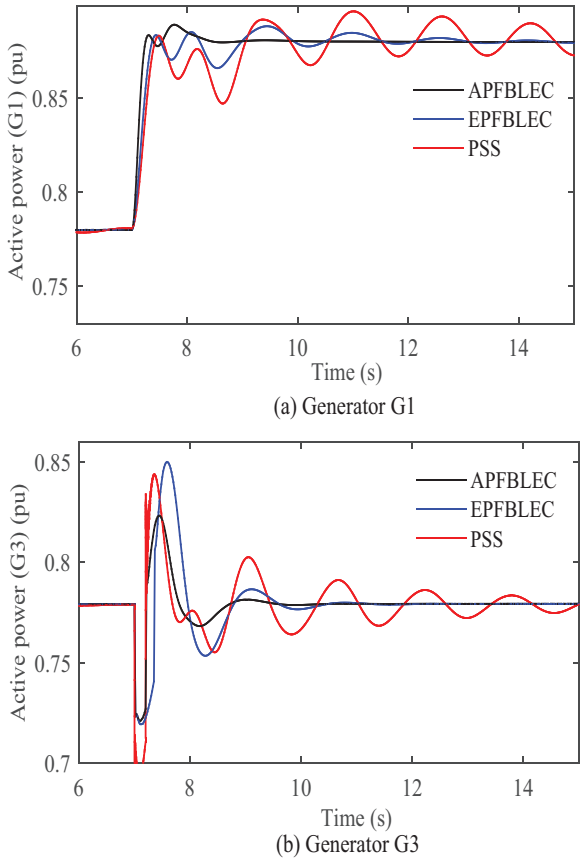

FIGURE 21 Output active power of G1 and G3 with external noises to mechanical power inputs of these generators

are shown in Figures 25–27, respectively. From these simulation results, it can be seen that the steady-state operation of the large power system with the designed controller is maintained within the timeframe of transient stability, i.e. 2 s. But the existing controller is unable to achieve the steady state within the desired time and hence, it can be said that the designed APFBLEC is effective for all systems irrespective of the dimensions of the system.

7 | CONCLUSION

Adaptive excitation controllers are designed for partial feedback linearized synchronous generators in multimachine power systems which alleviate the parameter sensitivity problems in the existing feedback linearization technique while ensuring the stability of the whole system against different types of large disturbances. The stability sensitive parameters which appear in the partial feedback linearizing excitation control laws estimated through adaptation laws as these are assumed as completely unknown. The estimated values of the stability sensitive parameters are used during the implementation of the controller. The Lyapunov stability theory ensures the overall stability of multimachine power systems with the designed parameter adaptation and excitation control laws. The designed

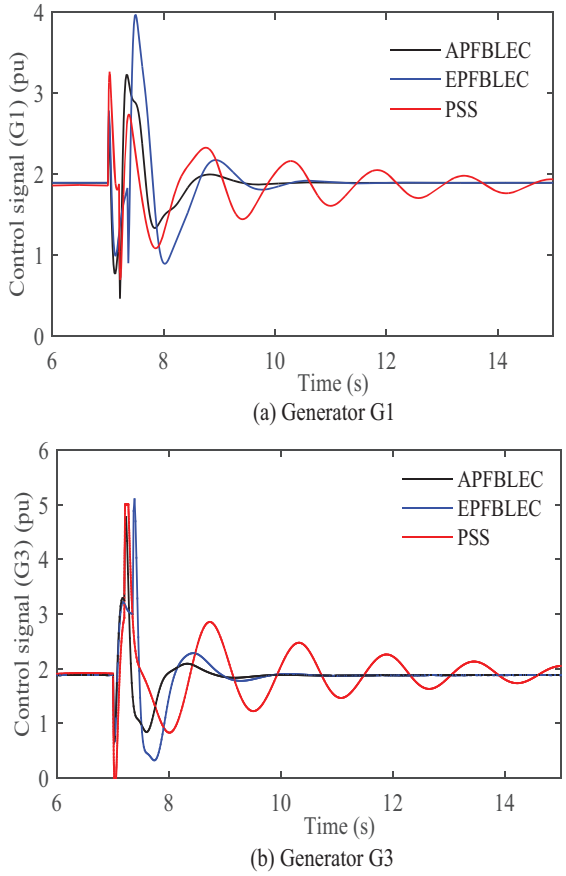

FIGURE 22 Control signals of G1 and G3 with external noises to mechanical power inputs of these generators

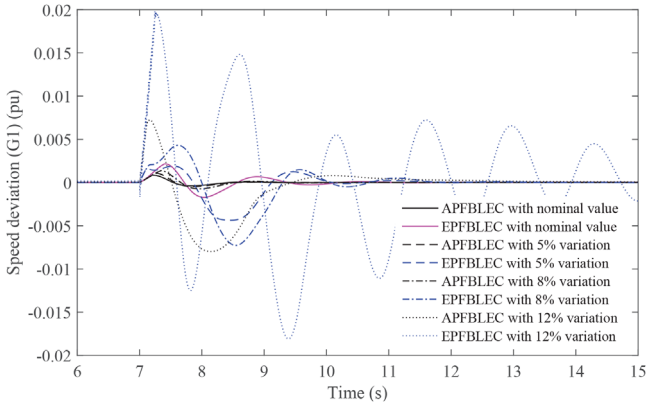

FIGURE 23 Speed deviation of G1 with variations in parameters

controllers are implemented on two different multimachine power systems and detailed simulation results are presented in order to investigate the performance of the designed excitation controllers under different operating conditions. Simulation results clearly depict the superiority of the designed control scheme regardless of the parameter variations under different operating conditions and different types of faults with longer duration. Furthermore, the designed controller ensures better

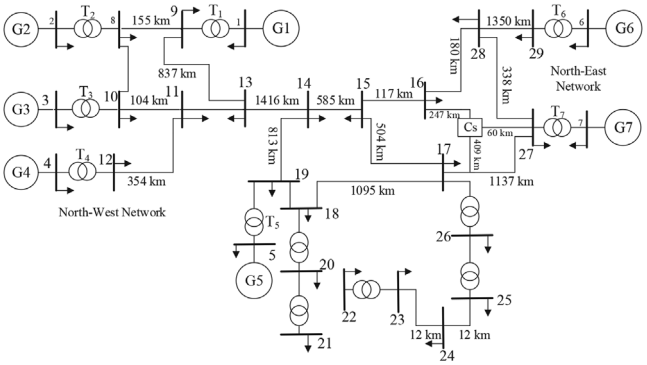

FIGURE 24 Test system: three-area seven machine 29-bus network

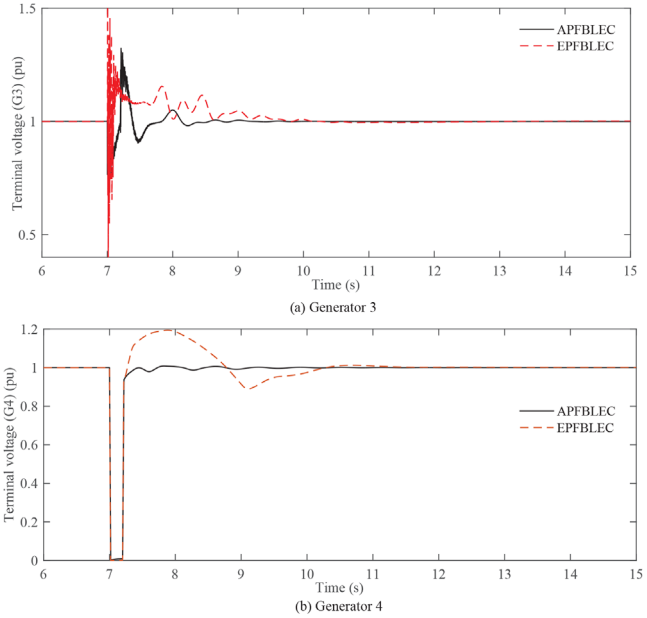

FIGURE 25 Terminal voltages of G3 and G4 while applying a symmetrical short-circuit fault at the terminal of G4

percentage overshoot and settling time along with the larger stability margin for almost all responses as compared to existing controllers in the similar frame. The main challenge in the implementation of this backstepping controller into a practical system is the selection of gain parameters. However, this can easily be overcome by selecting these gains in the hardware-in loop (HIL) platform before the practical implementation. Since there are lot of uncertainties due to the integration of renewable energy sources, the developed control scheme in this paper will create a new direction to control these renewable energy sources. The partial feedback linearizing adaptive backstepping approach as developed in this paper will enable the estimation of unknown parameters in renewable energy applications. Therefore, future works will investigate the utilization of this control scheme with the integration of renewable energy sources into conventional power systems.

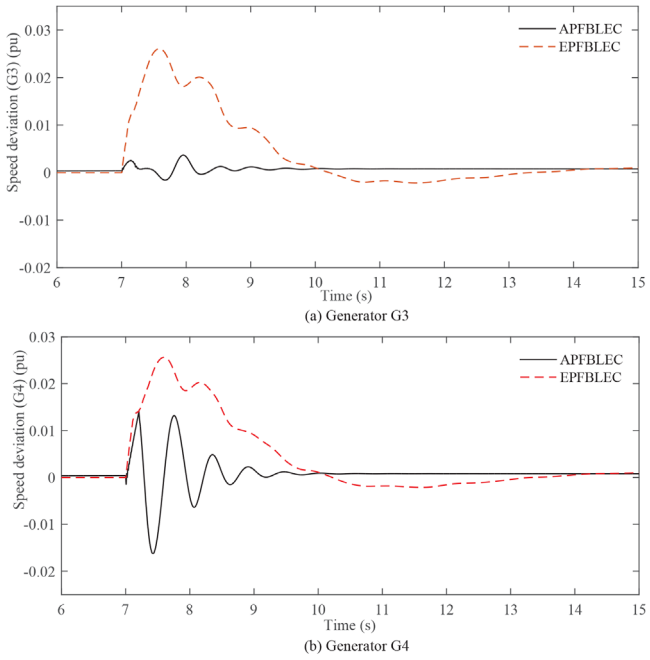

FIGURE 26 Speed deviations of G3 and G4 while applying a symmetrical short-circuit fault at the terminal of G4

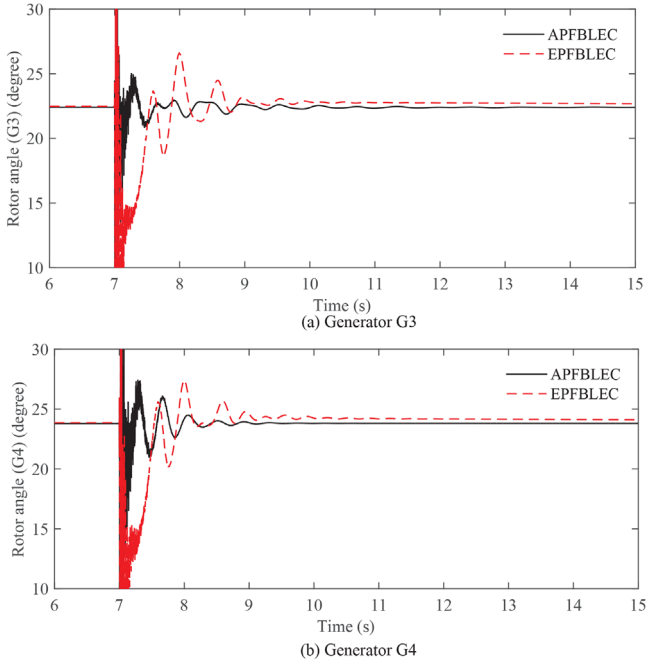

FIGURE 27 Rotor angles of G3 and G4 while applying a symmetrical short-circuit fault at the terminal of G4

NOMENCLATURE

i	ith generator
δ_i	Rotor angle
ω_i	Measured speed
ω_{0i}	Synchronous speed
D_i	Damping coefficient
H_i	Inertia constant
P_{mi}	Mechanical input
P_{ei}	Output active power
E'_{qi}	Quadrature-axis transient voltage
E_{qi}	Quadrature-axis voltage
E_{fdi}	Field excitation voltage
T_{doi}	Direct-axis open-circuit time constant
x'_{di}	Direct-axis transient reactance
x_{di}	Direct-axis synchronous reactance
Q_{ei}	Output reactive power
G_{ii}	Self-conductance
B_{ii}	Self-susceptance
G_{ij}	Conductance between ith and jth lines
B_{ij}	Susceptance between ith and jth lines
I_{di}	Direct-axis current
I_{qi}	Quadrature-axis current
V_{ti}	Terminal voltage
x	States of non-linear system
$f(x)$	Non-linear function of states related to the system
$g(x)$	Non-linear function of states related to the input
u	Control input of non-linear systems
y	Output of non-linear systems
$h(x)$	Output function
z	State obtained from non-linear coordinate transformation
L	Lie derivative
v_i	Virtual linear control input for ith generator
θ	Unknown parameters
$\hat{\theta}$	Estimator for unknown parameters
$\tilde{\theta}$	Estimation error for unknown parameters
W	Control Lyapunov function
e	Error
γ	Adaptation gains
k	Tuning parameters

REFERENCES

1. Hu, X., et al.: Integrated optimization of battery sizing, charging, and power management in plug-in hybrid electric vehicles. IEEE Trans. Control Syst. Technol. 24(3), 1036–1043 (2016)
2. Kundur, P.: Power System Stability and Control. McGraw-Hill, New York (1994)
3. Mahmud, M.A., et al.: Robust partial feedback linearizing excitation controller design for multimachine power systems. IEEE Trans. Power Syst. 32(1), 3–16 (2017)
4. Liu, H., Hu, Z., Song, Y.: Lyapunov-based decentralized excitation control for global asymptotic stability and voltage regulation of multimachine power systems. IEEE Trans. Power Syst. 27(4), 2262–2270 (2012)
5. Zhao, P., et al.: Improved synergetic excitation control for transient stability enhancement and voltage regulation of power systems. Int. J. Electr. Power Energy Syst. 68, 44–51 (2015)
6. Marco, F.J.D., Martins, N., Rezende-Ferraz, J.C.: An automatic method for power system stabilizers phase compensation design. IEEE Trans. Power Syst. 28(2), 997–1007 (2013)
7. Gurrala, G., Sen, I.: Power system stabilizers design for interconnected power systems. IEEE Trans. Power Syst. 25(2), 1042–1051 (2010)
8. Ma, J., Wang, H.J., Lo, K.L.: Clarification on power system stabiliser design. IET Gener. Transm. Distrib. 7(9), 973–981 (2013)

9. Mahmud, M.A.: An alternative LQR based excitation controller design for power system to enhance small-signal stability. Int. J. Electr. Power Energy Syst. 63, 1–7 (2014)
10. Hourfar, F., et al.: Mixed H_∞/passivity controller design through LMI approach applicable for waterflooding optimization in the presence of geological uncertainty. Comput. Chem. Eng. 142, 107055 (2020)
11. Chang, L., Jing, Y., Liu, Y.: Design of adaptive H_∞ controller for power system based on prescribed performance. ISA Trans. 100, 244–250 (2020)
12. Mahmud, M.A., Hossain, M.J., Pota, H.R.: Effect of large dynamic loads on power system stability. Int. J. Electr. Power Energy Syst. 44(1), 357–363 (2013)
13. Guo, G., Wang, Y., Hill, D.J.: Nonlinear output stabilization control for multimachine power systems. IEEE Trans. Circuits Syst. I Fundam. Theory Appl. 47(1), 46–53 (2000)
14. Hao, J., et al.: Nonlinear decentralized disturbance attenuation excitation control for power systems with nonlinear loads based on the Hamiltonian theory. IEEE Trans. Energy Convers. 22(2), 316–324 (2007)
15. Dib, W., et al.: A "globally" convergent controller for multimachine power systems using structure-preserving models. IEEE Trans. Autom. Control 54(9), 2179–2185 (2009)
16. Gan, D., Qu, Z., Cai, H.: Multi machine power system excitation control design via theories of feedback linearization control and nonlinear robust control. Int. J. Syst. Sci. 31(4), 519–527 (2000)
17. King, C.A., Chapman, J.W., Ilic, M.D.: Feedback linearizing excitation control on a full-scale power system model. IEEE Trans. Power Syst. 9(2), 1102–1109 (1994)
18. Akhrif, O., et al.: Application of a multivariable feedback linearization scheme for rotor angle stability and voltage regulation of power systems. IEEE Trans. Power Syst. 14(2), 620–628 (1999)
19. Mahmud, M.A., et al.: Partial feedback linearizing excitation controller for multimachine power systems to improve transient stability. IEEE Trans. Power Syst. 29(2), 561–571 (2014)
20. Mahmud, M.A., Hossain, M.J., Pota, H.R.: Transient stability enhancement of multimachine power systems using nonlinear observer-based excitation controller. Int. J. Electr. Power Energy Syst. 58, 57–63 (2014)
21. Mahmud, M.A., Pota, H.R., Hossain, M.J.: Full-order nonlinear observer-based excitation controller design for interconnected power systems via exact linearization approach. Int. J. Electr. Power Energy Syst. 41(1), 54–62 (2012)
22. Kenne, G., et al.: An improved direct feedback linearization technique for transient stability enhancement and voltage regulation of power generators. Int. J. Electr. Power Energy Syst. 32, 809–816 (2010)
23. Mahmud, M.A., Hossain, M.J., Pota, H.R.: Investigation of critical parameters for power systems stability with dynamic loads. In: Proc. of EEE PES General Meeting, pp. 1–6 (2010)
24. Roy, T.K., et al.: Non-linear adaptive coordinated controller design for multimachine power systems to improve transient stability. IET Gener. Transm. Distrib. 10(13), 1–11 (2016)
25. Australian Energy Market Operator: Notice of Inertia and Fault Level Shortfalls in Tasmania. AEMO (2019)
26. Wang, Y., Hill, D.J.: Robust nonlinear coordinated control of power systems. Automatica 32(4), 611–618 (1996)
27. Huerta, H., Loukianov, A.G., Cañedo, J.M.: Robust multimachine power systems control via higher order sliding modes. Int. J. Electr. Power Energy Syst. 81(7), 1602–1609 (2011)
28. Huerta, H., Loukianov, A., Canedo, J.M.: Decentralized sliding mode block control of multimachine power systems. Int. J. Electr. Power Energy Syst. 31(1), 1–11 (2010)
29. Karim, A., Feliachi, A.: Decentralized adaptive backstepping control of electric power systems. Electr. Power Syst. Res. 78(3), 484–493 (2008)
30. Yan, R., et al.: A power system nonlinear adaptive decentralized controller design. Automatica 46(2), 330–336 (2010)
31. Shen, T., et al.: Adaptive nonlinear excitation control with L2 disturbance attenuation for power systems. Automatica 39, 81–89 (2003)
32. Wang, K., et al.: Nonlinear robust adaptive excitation controller design in power systems based on a new back-stepping method. IET Control Theory Appl. 4(12), 2947–2957 (2010)
33. Verrelli, C.M., Damm, G.: Robust transient stabilisation problem for a synchronous generator in a power network. Int. J. Control 83(4), 816–828 (2010)
34. Roy, T.K., et al.: Robust nonlinear adaptive backstepping excitation controller design for rejecting external disturbances in multimachine power systems. Int. J. Electr. Power Energy Syst. 84, 76–86 (2017)
35. Roy, T.K., Mahmud, M.A., Oo, A.M.T.: Robust adaptive backstepping excitation controller design for higher-order models of synchronous generators in multimachine power systems. IEEE Trans. Power Syst. 34(1), 40–51 (2019)
36. Su, Q., Dong, F., Li, J.: Improved nonlinear robust adaptive backstepping controller design for generator excitation systems. IEEE Access 7, 83187–83197 (2019)
37. Poursamad, A.: Adaptive feedback linearization control of antilock braking systems using neural networks. Mechatronics 19, 767–773 (2009)
38. Fregene, K., Kennedy, D.: Stabilizing control of a high-order generator model by adaptive feedback linearization. IEEE Trans. Energy Convers. 18(1), 149–156 (2003)
39. Mahmud, M.A., Hossain, M.J., Pota, H.R.: Selection of output function in nonlinear feedback linearizing excitation control for power systems. In: Proc of Australian Control Conference (AUCC), pp. 458–463 (2011)
40. Lu, Q., Sun, Y., Mei, S.: Nonlinear Control Systems and Power System Dynamics. Kluwer Academic Publishers, Boston (2001)

How to cite this article: Roy TK, Mahmud MA, Shen WX, Oo AT. A non-linear adaptive excitation control scheme for feedback linearized synchronous generations in multimachine power systems. *IET Gener Transm Distrib*. 2021;15:1501–1520.
https://doi.org/10.1049/gtd2.12118